Similarity of Hand Muscle Synergies Elicited by Transcranial MagneticStimulation and Those Found During Voluntary Movement

Running head: TMS-Elicited and Voluntary Hand Muscle Synergies

Mathew Yarossi[1,2*], Dana H. Brooks[2], Deniz Erdoğmuş[2], Eugene Tunik[1,2]

[1]*Department of Physical Therapy, Movement and Rehabilitation Science, Northeastern University, Boston, USA*

[2]*SPIRAL Center, Department of Electrical and Computer Engineering, Northeastern University, Boston, USA*

[*]Department of Physical Therapy, Movement and Rehabilitation Science, 404 Robinson Hall, Northeastern University, 360 Huntington Ave, Boston, MA 02115, USA

Email address: m.yarossi@northeastern.edu (Mathew Yarossi)

Abstract

Converging evidence in human and animal models suggests that exogenous stimulation of the motor cortex (M1) elicits responses in the hand with similar modular structure to that found during voluntary grasping movements. The aim of this study was to establish the extent to which modularity in muscle responses to transcranial magnetic stimulation (TMS) to M1 resembles modularity in muscle activation during voluntary hand movements involving finger fractionation. EMG was recorded from eight hand-forearm muscles in nine healthy individuals. Modularity was defined using non-negative matrix factorization to identify low rank approximations (spatial muscle synergies) of the complex activation patterns of EMG data recorded during high density TMS mapping of M1 and voluntary formation of gestures in the American Sign Language alphabet. Analysis of synergies revealed greater than chance similarity between those derived from TMS and those derived from voluntary movement. Both datasets included synergies dominated by single intrinsic hand muscles presumably to meet the demand for highly fractionated finger movement. These results suggest corticospinal connectivity to individual intrinsic hand muscles may be combined with modular multi-muscle activation via synergies in the formation of hand postures.

New and Noteworthy: This is the first work to examine the similarity of modularity in hand muscle responses to transcranial magnetic stimulation (TMS) of the motor cortex and that derived from voluntary hand movement. We show that TMS-elicited muscle synergies of the hand, measured at rest, reflect those found in voluntary behavior involving finger fractionation. This work provides a basis for future work using TMS to investigate muscle activation modularity in the human motor system.

Keywords: transcranial magnetic stimulation (TMS), muscle synergy, motor cortex

Introduction

The coordination and flexibility of motor commands needed to carry out purposeful everyday hand movements requires controlling a highly redundant system with numerous degrees of freedom (1-3). The observation that voluntary behavior can be well characterized by a low dimensional linear basis set has generated the hypothesis that movements may be generated from a small set of flexible modules, commonly referred to as motor synergies (4, 5). The most common theoretical conceptualization of motor synergies, whether they are expressed as muscle activation (muscle synergies) or kinematics (postural synergies), is that they form a small set of basic units of motor output that can be flexibly (and usually linearly) combined to generate a wide range of complex motor behaviors (6, 7). Though this definition remains controversial (3), it has nevertheless been used extensively in the effort to understand the organization of neural systems, applied to clinical populations as a diagnostic tool to explain pathological movement patterns (often referred to as ”abnormal synergies” by clinicians), and offers an explicit hypothesis to guide the design of investigations into motor modularity (8). Synergy analysis has been used to describe patterns of force generation (9), movement kinematics (10), and hand postures (5, 11). There is now considerable evidence from a broad range of tasks that the voluntary activity of multiple muscles can be well-approximated by a smaller number of muscle synergies in frogs (12), cats (13), monkeys (14), and in both the upper (15-17) and lower limbs of humans (18).

However, the ability to accurately describe voluntary activity using a low dimensional representation does not provide evidence that motor synergies exist as an organizational structure within the nervous system. Alternative hypotheses have suggested that constraints of the task (19) and the musculoskeletal plant (20) may explain the observed covariance captured in the construction of a low dimensional representation of volitional motor output. More compelling evidence that muscle synergies exist as an organizational structure within the nervous system, is rooted in the observation that adaptation to a “virtual surgery” to perturb the innate mapping between muscle activity and force

is slower when the perturbation is not compatible with the synergies than when it is (21). The most direct evidence in support of the framework for modular organization in the motor system stems from electrical microstimulation studies in animal models. Whether applied intraspinally (9, 22), transcutaneously (1), or intracortically (14, 23-26), localized suprathreshold microstimulation that lasts several hundred milliseconds can evoke complex multijoint forces which generally drive the animal's limb toward an invariant posture. The appeal and clear advantage of using microstimulation is that it serves as a causal probe into the motor system. However, the validity of microstimulation as a causal probe for studying neural organization (and associated function) is critically dependent on the assumption that artificially elicited motor output (whether it be muscle activation, force, or movement) is a valid model of voluntary behavior. A number of animal-based studies have investigated this question and reported marked similarity between synergies observed during voluntary behavior and those elicited either by spinal microstimulation (e.g., force-fields: (9)) or cortical microstimulation (e.g., kinematics: (23), EMG: (14, 24, 25).

Due to the relative difficulty of invasive direct cortical stimulation in humans, comparing modularity between stimulus-evoked and voluntarily-produced outputs has been sparsely studied in people. Transcranial magnetic stimulation (TMS) offers a non-invasive alternative to invasive microstimulation and has been leveraged to show that TMS-induced finger movements resemble end-postures of voluntary grasping movements, and that a small subset of hand postures was sufficient to accurately reconstruct these movements (27). In line with these findings, it has also been shown that individuals who are expert musicians have movement patterns, evoked by TMS to the motor cortex (M1) at rest, that are reflective of the specific instrument that a given musician is skilled at playing, and moreover that those patterns are different from those elicited in non-musically trained individuals (28). This line of work suggests that the modularity in the motor system observed using TMS may be informative about the probability distribution of neural activation patterns that underlie the natural statistics of individual human behavior.

The studies described above focused on overt movements (postural synergies), rather than on the underlying muscular patterns of activation, leaving untested the validity of TMS-elicited *muscle* synergies for understanding behavior. Given that muscle responses to TMS, commonly referred to as motor evoked potentials (MEPs), have shown diagnostic and prognostic value in a wide range of pathologies (29-31), and are considerably easier to collect and analyze in a clinical setting than movement kinematics, it is critical to determine the degree to which artificially-elicited muscle activation patterns are a valid marker of modular organization of volitional behavior. The current study is a first step in examining the relevance of TMS-elicited muscle synergies to voluntary muscle activation in a cohort of healthy individuals, with the goal that this work could serve as a foundation for understanding TMS as a tool for investigation of motor system organization. Figure 1 presents a conceptual overview of the study design. We investigated three questions. First, we asked whether multi-muscle MEPs in the hand and forearm, acquired at rest using a TMS mapping protocol spanning the sensorimotor cortices, can be described by a low-dimensional space such as that previously used by others to represent synergies. Affirming this to be the case, we investigated the ecological validity of TMS-elicited hand muscle synergies by quantifying the similarity between them and those identified during voluntary movement. Finally, we examined the extent to which TMS-elicited and voluntary hand muscle synergies are invariant across a sample of healthy individuals.

2. Methods

2.1 Subjects

All protocols were conducted in conformance with the Declaration of Helsinki and were approved by the Institutional Review Board of Rutgers Biomedical Health Sciences. Eight healthy subjects (3 female, 37.6±11.8 years) participated after providing institutionally approved written informed consent. All subjects were right-hand dominant according to the Edinburgh handedness inventory (32), free of neurological or orthopedic conditions that could interfere with the experiment, and met

136 inclusion/exclusion criteria to receive TMS (33). All subjects were naive to American Sign Language
137 Alphabet (ASL) prior to participation.
138
139 **2.2 Experimental Setup**
140
141 For TMS and voluntary assessments, subjects were seated comfortably with the right elbow and
142 forearm sup- ported in an arm trough so that the wrist was free to move. The left upper limb was
143 positioned to rest comfortably on an arm rest. Surface electromyography (EMG) (Delsys Inc., Natick, MA)
144 was recorded at 2000 Hz (common mode rejection ratio >80 dB, 99.99% Ag, built-in 20–450 Hz
145 bandpass filter) from eight muscles: the first dorsal interosseus (FDI), extensor indicus (EI),
146 abductor pollicis brevis (APB), adductor digiti minimi (ADM), flexor digitorum superficialis (FDS),
147 extensor digitorum (EDC), flexor carpi radialis (FCR), and extensor carpi radialis (ECR) of the right
148 upper limb. A combination of Delsys Trigno Mini sensors (FDI, EI, APB, ADM) and Delsys Trigno
149 standard sensors (FDS, EDC, FCR, ECR) were used. Locations of the muscles recorded can be found
150 in Fig. 2.
151
152 2.3 Neuronavigated TMS Mapping
153
154 To ensure spatial TMS precision, frameless neuronavigation (Brainsight, Rogue Research) was
155 used to co-register the subjects' head position to a 3D cortical surface rendering of a canonical high-
156 resolution anatomical MRI scan. The TMS coil (Magstim Rapid2, D70 70mm figure-of-eight coil) was
157 held tangential to the scalp with the handle posterior 45° off the sagittal plane (34). All TMS
158 measures were collected with the subject resting comfort-ably in the position described above, with the
159 wrist and fingers relaxed in a semi-prone position. The locus of the cortical hotspot for the right FDI
160 was established by per- forming a coarse mapping of the left hemisphere starting at a location
161 approximately 5 cm lateral to the vertex (35). Muscle responses to TMS were described by the size of
162 the motor evoked potential (MEP), quantified as the peak-to-peak amplitude of the EMG signal during

163 a window from 10 to 40ms following the TMS pulse. The stimulator intensity was set to a level
164 sufficient to produce visible and reliable MEPs. The hotspot was determined by sampling MEPs at
165 different loci to identify the location that produced the largest and most consistent MEP amplitudes
166 (36). This method has been shown to have high intra- and inter-experimenter reliability, and has been
167 cross-validated with fMRI for finding the site of greatest activation for a given muscle (37). Following
168 determination of the FDI hotspot, resting motor thresh- old (RMT), was determined as the minimum
169 intensity required to elicit MEPs >50μV in the FDI muscle on 50% of 6 consecutive trials.
170
171 For TMS mapping, 297 to 299 stimulations (4s ISI, 110% FDI RMT) were delivered over a
172 6×6cm area centered on the FDI hotspot. TMS mapping was conducted with the subject at rest,
173 verified by visual inspection of background EMG. Real time visual feedback of the MEP time traces
174 for all muscles and neuronavigated coil position provided to the experimenter during the testing
175 session maximized the map information obtained by allowing for increased density of points in
176 excitable and border regions, with less attention given to far-away non-responsive areas (28, 30, 38,
177 39). Care was taken to ensure mapping included the full extent of the excitable area for all recorded
178 muscles. This approach has been previously described in detail by our group (30, 40) and others (38),
179 and non-gridded approaches have been shown to produce similar results to traditional gridded
180 mapping (40-42). For each stimulation, MEP amplitudes were recorded from the 8 muscles and used
181 for further analysis. Prior to synergy extraction, MEP amplitudes from each muscle were concatenated
182 across all simulations and normalized to the respective muscle's maximum MEP value.
183
184 **2.4 Voluntary Motor Task**
185
186 While seated in the same setup, and in the same session, subjects were instructed to shape
187 their right hand into each of 32 static letters and numbers of the ASL posture set (17), mimicking each
188 posture shown on a computer screen one at a time. Subjects were given 2s to form each posture, and
189 instructed to statically maintain the posture for 6s. Subjects performed each posture 3 times (96 total

trials). EMG data were filtered using a fourth-order Butterworth bandpass filter with cutoff frequencies of 10 Hz (Low) and 300 Hz (High). Root mean square (RMS) EMG from each muscle in the window 5.5–7.5s following cue, during the static hold period, was used for analysis. Prior to synergy extraction (see below), the windowed RMS EMG data from each muscle were concatenated across the 96 trials and normalized to the maximum of the respective muscle's RMS EMG value.

2.5 Extraction of muscle synergies

Muscle synergies were extracted separately from voluntary EMGs (VOL) in the ASL task and from MEP amplitudes in the TMS mapping task (TMS) using standard non-negative matrix factorization (NMF) (43), as described previously (44, 45). Several other dimensionality reduction methods, such as principle components analysis (PCA) and independent components analysis (ICA), have been utilized for the purpose of muscle synergy analysis (45). NMF has emerged as the most common technique primarily because the non-negativity constraint is a useful attribute for identifying physiologically meaningful synergies given the inherent non-negativity of muscle activation (7). For this reason, and to permit comparison to the vast majority of the relevant literature, NMF was chosen for dimensionality reduction in this study. In depth discussion of the conceptual and mathematical framework for muscle synergy analysis has been covered extensively in previous reports (16, 45-47). Briefly, we describe our application of NMF mathematically as:

$$M_{VOL} = B_{VOL} \cdot A_{VOL} + \varepsilon$$
$$M_{TMS} = B_{TMS} \cdot A_{TMS} + \varepsilon \qquad (1)$$

where M_{VOL} is matrix of RMS EMG of size m muscles by p postures and M_{TMS} is a matrix of MEP amplitudes of size m muscles by s stimulations, describing the motor response in each task. B_{VOL} and B_{TMS} are low rank matrices, of column size N_{VOL} and $N_{TMS,}$ respectively, containing the time-invariant

217 non-negative basis vectors (of length m) in muscle space. A_{VOL} and A_{TMS} are the N_{VOL} by p and N_{TMS}
218 by s matrices representing the per trial activation coefficients. For any pre-specified rank (N_{VOL} or
219 N_{TMS}), NMF finds the corresponding B and A by minimizing the squared norm (variance) of the
220 residual, ε, under the assumption that it follows a Gaussian distribution and is zero mean and
221 uncorrelated. The algorithm iteratively updates the model parameters until R^2, referred to in the
222 literature as the proportion of variance explained or the fraction of variance accounted for, increased
223 by less than 0.001 over ten iterations, where R^2 is given by:
224

$$R^2 = 1 - RSS/SST = 1 - \frac{\sum ij \left(M_{i,j} - (BA)_{i,j}\right)^2}{\sum ij \left(M_{i,j} - \bar{M}\right)^2}$$

225 (2)
226

227 where RSS is the residual sum of squares, SST is the total sum of squares, the i, j subscript denotes
228 the corresponding entry of the matrix, and $\bar{M}$ is the average over all entries of M (48). To determine the
229 number of synergies to include, NMF was conducted with candidate N_{VOL} and N_{TMS} values that ranged
230 from 1 to 8 (eight being the total number of muscles that we recorded activity from and which would
231 allow for a perfect reconstruction). For each such value of (N_{VOL} and N_{TMS}), the set of synergies (B_{VOL}
232 and B_{TMS}) able to explain the most variation (the largest R^2)) over 100 repetitions of the algorithm were
233 chosen for further analysis (25). Finally, a fixed N_{VOL} and N_{TMS} were chosen as the minimum number of
234 synergies needed to reconstruct 90% of the observed variance in the data from which they were
235 derived (15). As a control comparison, this process was repeated for unstructured MVOL and MTMS
236 generated by randomly shuffling the original data across both muscles and trials (m, p) 1000 times in
237 order to estimate chance level R^2 values (15). Throughout the remainder of the manuscript N_{VOL}, N_{TMS},
238 B_{VOL}, B_{TMS}, A_{VOL}, and A_{TMS} refer to the selected synergies that minimally satisfied the 90% R^2 criterion
239 (15).
240

241 **2.6 Quantifying Similarity of TMS and VOL Synergies**

In this work, we are interested in quantifying the similarity between synergies both as a subspace, that is as a collection or set of synergies, and also on an individual synergy-by-synergy basis. The former measures whether the synergies taken as a whole describe similar combinations of muscle activations, while the latter, which is stricter, measures the similarity of the muscle co-activation patterns. We quantified the correspondence between the sets of synergies underlying TMS and VOL muscle activations by using the cross-reconstruction R^2_{CR} as a global measure of synergy set similarity (15). The cross-reconstruction R^2_{CR} was calculated by solving the non-negative least squares estimation problem in the form:

$$argmin_{\hat{A}} \parallel B\hat{A} - M \parallel_F^2 \; subject \; to \hat{A} \geq 0 \tag{3}$$

$$R^2_{CR} = 1 - RSS/SST = 1 - \frac{\sum ij \left(M_{i,j} - \left(B\hat{A}\right)_{i,j}\right)^2}{\sum ij \left(M_{i,j} - \bar{M}\right)^2} \tag{4}$$

Here $\hat{A}$ represents the activation coefficient matrix of non-negative values that provides the best fit of a synergy set *B* from one experiment to dataset *M* from another, *F* represents the Frobenius matrix norm, and ≥ is taken elementwise. R^2_{CR} was calculated separately for the cases of (B_{VOL}, M_{TMS}) and (B_{TMS}, M_{VOL}), as described in Eq. 4. Chance level for R^2_{CR} was again determined by Monte Carlo simulation on synergies constructed by randomly shuffling muscle identity. Specifically, when reconstructing M_{TMS}, the synergies in B_{VOL} were shuffled (1000 times), and when reconstructing M_{VOL} the synergies in B_{TMS} were shuffled (1000 times), in order to generate chance level distributions to compare against actual cross-reconstruction values. Cross-reconstruction R^2_{CR} for each case was then compared at the group level using a paired sample *t*-test ($P < 0.05$). To verify that differences between R^2 and R^2_{CR} seen at the group level are not simply the result of noise affecting the synergy

decomposition, we used cross-validation to obtain values for R^2 and R^2_{CR} individually for each participant. Cross-validation was performed by generating 10 different data subsets comprised of 60% of the trials (randomly sampled), extracting synergies from each subset using the same NMF procedure that was used on the full set, and using those synergies to reconstruct (again using the same procedure as was described for the full set) the remaining 40% of trials (cross-validated global reconstruction R^2) (15). This procedure was repeated for each dataset (TMS and VOL). Cross-validated global cross-reconstruction R^2_{CR} was calculated using the synergies extracted from each of the 10 subsets to reconstruct the remaining 40% of trials in the other condition for that participant.

To carry out the per-synergy comparison, we identified a paired ordering of synergies between TMS and VOL experiments using a greedy search procedure for each subject. To do so, dot products were computed between all possible pairs of VOL and TMS synergies, and the best-matching pair was defined as the one with the highest dot product. This pair was then removed from the set, and the next best matching pair was selected as highest dot product among the remaining synergy pairs. This process continued until there were no more unpaired synergies left in the set (1). Chance level for testing the significance of each matched pair was determined by Monte Carlo simulation on synergies constructed by randomly shuffling muscle identity. For each participant, 5,000 random synergies for each set of 5 VOL and TMS synergies (1,000 per synergy) were constructed by randomly shuffling the muscle weights from the original muscle synergies. Next, the dot products of all possible pairs of random synergies from the two datasets (25×10^6 pairs in total) were calculated. The 95th percentile of the distribution of dot products was then set as the threshold to compare whether matched pairs of TMS and VOL synergies were statistically significant ($P = 0.05$), indicating a similar synergy structure.

2.7 Quantifying Population Level Similarity of Synergies

To quantify the overall similarity of muscle synergies derived from either TMS or VOL data, group mean synergies for each task (B_{VOL}^{Group}, B_{TMS}^{Group}) were generated by arbitrarily selecting one subject's synergies as a template, to which the synergies from the remaining subjects were matched using the greedy algorithm described above and then group averaged (15). We verified that group mean synergies were not sensitive to the choice of template. To assess the consistency of individual synergies across the sample, the dot product between synergies from each subject and the corresponding group mean synergies were calculated. Finally, similarity between individual synergies in B_{VOL}^{Group} and B_{TMS}^{Group} were calculated, again using the same greedy search procedure.

To quantify the incidence in the population of particular synergies across the two conditions a clustering analysis was performed. TMS and Voluntary synergies (5 per condition) for all subjects (n = 8) were pooled (80 synergies total) and grouped using hierarchical cluster analysis with Euclidean distance as the similarity measure. The clustering procedure was performed by applying the Matlab statistics-toolbox functions *pdist* (Minkowski distance option; p = 2), linkage (ward option), and cluster to the pooled synergy matrix. The number of clusters was determined as the minimum number of clusters partitioning the synergies such that there was not more than one synergy in each cluster from a given subject per condition (i.e., single subject could contribute a single TMS synergy and/or a single VOL synergy to the same cluster) (44, 49, 50).

3 Results

TMS mapping was well-tolerated by all subjects and no adverse effects of stimulation were reported. Resting motor thresholds, stated as a percentage of maxi- mum stimulator output (% MSO), for the eight participants were: S1 (59), S2 (50), S3 (49), S4 (39), S5 (42), S6 (43), S7 (50), and S8 (42). Fig. 3*A*. depicts EMG traces showing MEPs recorded during TMS mapping, and Fig. 3*B*. depicts voluntary EMG recorded during the ASLtask for a representative participant.

****

Insert Fig. 3

****

3.1 Five Synergies Reliably Reconstructed TMS-Elicited and Voluntary Muscle Activation Patterns

We first investigated whether multi-muscle evoked potentials elicited during TMS based mapping of M1 hand topography could be described by a low- dimensional space that is similar in rank to that derived from volitional muscle activation. For TMS data 4.5± 0 .50 synergies and for VOL data 5.37± 0.51 synergies were the average number of synergies required to produce R^2 > 90% (Fig. 4). Five synergies were most often required to meet the 90% R^2 threshold in the 16 (8 subjects by 2 conditions) datasets (9 of 16), and resulted in average R^2 values of 93.2± 2.0% for TMS and 90.6± 3.1% for VOL, each of which was significantly greater than the estimated within dataset chance level (P < 0.05). For individuals who required either 4 or 6 synergies to meet the R^2 > 90% the addition of 1 synergy (from 4 to 5) or subtraction of one synergy (from 5 to 6) did not cause greater than a 5% change in R^2. Given these reconstruction results, 5 synergies were extracted from all datasets to facilitate within- and across- condition comparisons (14).

****

Insert Fig. 4

****

3.2 Similarity of TMS-Elicited and Voluntary Synergies

To evaluate the similarity of the subspace spanned by the set of TMS and VOL synergies, within-class reconstructions (with quantification by R^2) and cross-reconstructions (with quantification

by R^2_{CR}) for the 8 recorded muscles individually and collectively (global) were calculated for each subject. Individual muscle reconstructions including R^2 and R^2_{CR} values are shown for a single subject in Fig. 5, top panel, and group level muscle and global reconstruction R^2 and R^2_{CR} (labeled VE to encompass both measures) are shown in Fig. 5, bottom panel. Mean muscle R^2 across individuals was significantly different than chance for all muscles, and greater than 0.8 for all muscles tested with the exception of the EI for the voluntary task, indicating moderate to excellent reconstruction of individual muscle activity in both sets. Mean muscle R^2_{CR} across individuals, muscles and conditions ranged between .39 and .96, and cross-reconstruction of both TMS and VOL datasets was significantly different from chance for intrinsic hand muscles FDI and APB for. R^2_{CR} values for cross-reconstruction of TMS data from B_{VOL} for the ADM and ECR were also found to be significantly different from chance. Repeated measures ANOVAs with factors of Data Source (TMS, VOL) and Reconstruction Type (Within R^2, Cross R^2_{CR}) were used to test for main effects and interactions in the reconstruction of each data sets; results are summarized in Table 1. A significant main effect of Reconstruction Type was found for each muscle indicating cross-reconstruction fits using synergy bases from the other dataset were significantly lower than when bases were derived from within the dataset. For the FDI muscle there was also a significant main effect of Data Source ($F_{1,7}$ = 13.02, P = 0.009) and a significant Data Source by Reconstruction Type interaction ($F_{1,7}$ = 9.26, P = 0.019). For the FDI, post-hoc t-test with Bonferroni correction (α = 0.0125) for multiple comparisons revealed a significant difference between R^2 and R^2_{CR} for voluntary data (t_7 = 3.43, P = 0.011) but not TMS data (t_7 = 0.070, P = 0.504).

****

Insert Fig. 5

****

Global R^2 and $R_{CR}{}^2$ was found to be greater than the chance level for TMS and VOL datasets. There was significant main effect of Data Source ($F_{1,7}$ = 9.95, P = 0.016) and Reconstruction Type ($F_{1,7}$

372 = 138.80, $P < 0.001$), but no significant Data Source by Reconstruction Type interaction ($F_{1,7} = 3.98$, P
373 = 0.086). Post-hoc t-test with Bonferroni correction ($\alpha = 0.0125$) for multiple comparisons revealed a
374 significant difference in R^2 between TMS and VOL ($t_7 = 3.68$, $P = 0.008$), and a significant difference
375 between R^2 and R^2_{CR} for voluntary data ($t_7 = 9.542$, $P < 0.001$), and TMS data ($t_7 = 8.78$, $P < 0.001$).
376 Notably, there was no significant difference in the cross-reconstruction accuracy between datasets.
377
378 We observed two important results of individual participant cross-validation analysis of global
379 reconstruction R^2, as shown in Fig. 6. First, the within condition cross-validated global reconstruction
380 R^2 remained high (> 0.8) and often exceeded the 0.9 threshold that was used to determine the
381 number of synergies. Second, differences in cross-validated global reconstruction, depending on
382 whether synergies from the same condition (R^2) or the other condition (R^2_{CR}) were used for
383 reconstruction of EMG data, were similar to those found at the group level when the entire data set was
384 used.
385
386 Similarity of individual synergies extracted from TMS and from volitional movement were
387 quantified by the scalar product between synergies using a greedy search procedure to iteratively find
388 best-matching pairs as described. The resulting matched synergy pairs for all subjects are shown in
389 Fig. 7. There are 40 such parings (8 subjects by 5 synergies) out of which 21 were significantly
390 different from chance as determined by shuffling the muscle identities of the voluntary set.
391
392 **3.3 Consistency of Synergy Patterns Across Individuals**
393
394 Consistency of group mean synergy patterns across participants was evaluated for both TMS
395 and VOL datasets by grouping synergies as described above, using one subject picked at random as
396 the template, and then comparing the synergy coefficients for each muscle. Results are shown in Fig.
397 8*A*. Coefficients for each muscle are shown for each synergy as thin colored bars, and the mean and

398 standard deviations across the values for each muscle are shown with a thicker transparent bar with a
399 black outline. We computed an overall measure of consistency by calculating the dot product between
400 each individual and the corresponding group mean synergy, and then computed the mean and
401 standard deviation of those dot products across individuals. Average dot products between individual
402 subjects and the group mean exceeded 0.69 for all muscles, with standard deviations that were
403 consistently less than 0.2. Similarity (dot products) of TMS and VOL group mean synergies paired
404 using the greedy search procedure are shown in Fig. 8*B*. All group mean synergies were found to be
405 significantly greater than chance level ($P < 0.05$) as estimated by randomly shuffling the identities of
406 the group mean voluntary synergies. Generally, the FDI and the APB dominated one synergy each in
407 both the VOL and TMS conditions. Additionally, one synergy was dominated by a group of extrinsic
408 flexors (FCR and FDS) and one by a group of extrinsic extensors (EDC and ECR), suggestive of some
409 underlying functional groupings with respect to whole hand closing and opening respectively. Finally,
410 one synergy was comprised of the ADM and EI muscles, along with low level activation of the extrinsic
411 hand muscles in what could be best described as finger abduction synergy with coactivation to
412 stabilize the wrist.
413
414 The results shown in Fig. 8*A* indicate moderate homogeneity of muscle synergies derived from
415 TMS and voluntary EMG data across individuals, and similarity of population average TMS and VOL
416 synergies Fig. 8*B*. However, individual variation of synergies across conditions and individuals is
417 readily apparent. To better understand how synergies cluster across the population and conditions, we
418 pooled all synergies into a single set and grouped them using a cluster analysis. Fig. 9*A* illustrates the
419 identified clusters. Means for each cluster are represented by wide transparent bars with thick black
420 outlines and error bars (± 1*STD*), and individual subject synergies are shown as colored narrow bars.
421 Fig. 9*B* summarizes the incidence of each synergy for TMS and VOL data collections. Nine clusters
422 were identified with all clusters containing at least one TMS synergy and one VOL synergy (note that
423 this was not a constraint of the clustering method). FDI (Cluster 1) and the APB (Cluster 2) dominant
424 synergies were represented in TMS and VOL data sets for nearly all participants (one participant did

not contribute a TMS synergy to Cluster 2). Cluster 3 was characterized by grouping of the EI and ADM, resembling Synergy 5 in the group level analysis, contained 6 participants each for TMS and VOL data. Likewise, Cluster 4 displaying grouping of FDS and FCR and resembling Synergy 3 in the group level analysis, was present in 5 and 6 subjects for TMS and VOL synergies respectively. Differences between TMS and VOL are presented in Cluster 5 and 6. While both clusters are characterized by co- activation of EDC and ECR, Cluster 5 contains greater activation of the EI and is more often present in VOL synergies isolated higher activation of the ECR, EI and FDS respectively, were found in 3 or less participants for each data source and are indicative of the inter-subject variability found in the data.

Discussion

We used TMS to causally probe modularity in hand muscle activation. The results demonstrate that a NMF-derived low-dimensional representation was capable of describing patterns of covariance, consistent with current descriptions of muscle synergies. Most importantly, TMS-elicited muscle synergies bore a moderate-to-strong similarity to those produced from voluntary movement. Our findings complement those of Gentner and Classen (27), who found similarities in *postural* hand synergies extracted from grasping and TMS-elicited hand movements, and are in general agreement with animal investigations which have shown that cortical (25, 26) and spinal (9) stimulation-evoked muscle synergies resemble those extracted from voluntary motor behavior.

4.1 Comparison to TMS-Elicited Postural Synergies

The finding that TMS-elicited muscle synergies of the hand might resemble synergies found from voluntary behavior during a task requiring fractionated movement of the hand (forming postures of the ASL alphabet) is not entirely obvious from the findings of Gentner and Classen (27) who compared TMS-elicited postural synergies with those derived from grasping movements. Most notably,

452 in that study, TMS largely evoked composite movements of multiple fingers; isolated movements of
453 individual fingers, as would be required for fractionated control, were rarely observed.
454
455 To understand the differences between their work and ours, it is important to first consider
456 differences in postural (kinematic) and muscle synergies. While muscle synergies have been found to
457 be, at least partially, the source of kinematic synergies (51, 52) the relationship is undeniably complex.
458 Disentangling the mechanical coupling of movements caused by muscles acting across multiple digits
459 from the neural coupling (synergies) of muscles acting on different digits remains a challenging
460 problem (52, 53). However, it is possible to elicit single digit movements from TMS stimulation (54).
461 Therefore, a difference in the measured output, kinematics vs EMG, of TMS stimulation alone would not
462 explain why fractionated single muscle synergies were found in the present study yet single finger
463 movements were rarely found by Gentner and Classen (27).
464
465 We suggest that differences in the observation of finger individuation between our findings and
466 Gentner and Classen's are more likely the result of a difference in stimulus intensity used between that
467 study and ours. In order to evoke movements of the hand to produce postural synergies in their study, a
468 stimulation intensity of 130–140% of APB resting motor threshold was needed, as evoked movements
469 of the hand require greater intensity than the elicitation of MEPs (55). In contrast, TMS was applied at
470 110% of FDI resting motor threshold in our study. Given that the spread and depth of the TMS-induced
471 magnetic field increases monotonically with TMS output intensity, the extent of the cortical territory
472 activated or even the mechanism of cortical activation may differ between Gentner's and Classen's
473 study and ours. For example, it is known that TMS (using a coil type and orientation common to both
474 studies) at low intensities, just above threshold, preferentially activates intracortical horizontal fibers
475 (56), which are monosynaptic cortico-cortical connections, in an extended cortical network that is
476 presynaptic to the corticospinal projection neurons (57). At higher stimulus intensities (well above
477 threshold), additional mechanisms of activation occur, such as repetitive discharge of corticospinal
478 projection neurons through reverberating activation of excitatory microcircuits (58) and direct excitation

479 of the corticospinal projection neurons (57). Additional evidence of the effect of stimulus intensity on
480 corticospinal output and muscle recruitment stems from intracortical microstimulation studies in
481 primates (59). Hand/forearm muscles with the largest density of monosynaptic corticospinal
482 projections and least amount of divergence (i.e., projecting onto a single or a few muscles) are
483 preferentially activated at stimulation intensities just above motor threshold, while stronger stimulation
484 drives activation of both monosynaptic and multi-synaptic, involving divergent spinal or brainstem
485 interneurons, connections to musculature (22, 59).
486
487 It is possible that the higher intensity used by Gentner and Classen led to activation of a wider
488 intracortical network, differences in mechanisms of cortical activation, and recruitment of more
489 divergent projection neurons, producing predominately whole hand grasp-like responses, and a lack of
490 isolated finger movements akin to the "single muscle" synergies that we observed in our study.
491 Unfortunately, operational definitions of "low" and "high" intensity stimulation do not exist in the
492 literature and are likely to be highly individualized, requiring the direct measurement of the
493 corticospinal volley, which was beyond the scope of the current study. It is therefore impossible to
494 determine how different stimulation intensities (between our studies) impacted motor cortex activation.
495 Regardless of the underlying reason, our finding that single-muscle dominant synergies were found for
496 intrinsic hand muscles (most notably the primary movers of the index finger and thumb) but not for the
497 extrinsic muscles of the hand, are well-aligned with other empirical support for a critical role of the
498 primary motor cortex in individuated dexterous finger movements (53, 60, 61). In all, our findings
499 complement those of Gentner and Classen by showing that at lower levels of stimulation, multi-muscle
500 synergies that drive whole hand movements (such as the extensor, flexor, and abduction synergy seen
501 in both of our studies) may coexist along with single-muscle activation (identified in our study) which
502 may underlie fractionated control.
503
504 **4.2 Comparison to ICMS-Induced Synergies**
505

506 What does it mean that stimulation techniques with vastly different scales of stimulus resolution
507 (neural-level for ICMS and large population-level for TMS) both result in evoked responses that
508 resemble natural voluntary muscle activation? Here we contrast our findings to those of Overduin and
509 coworkers (25) in which trains of ICMS to macaque M1 evoked muscle synergies that strongly
510 resembled grasping toward a diverse set of objects. The mechanisms of neural activation evoked by
511 TMS and long train ICMS differ with regard to the number of neurons that are activated, the size of the
512 stimulated field, and the induction of activation due to stimulus repetition over a prolonged duration.
513 Yet despite these important differences, both Overduin and our group noted that the evoked synergies
514 largely mirrored those produced by volitional behavior. The most parsimonious explanation for this
515 agreement of findings across different species and scales of stimulation is that activation of the cortex
516 may be ultimately filtered through a vastly inter-connected divergent and convergent neural network in
517 the spinal cord, which has already been strongly tied to modularity in motor output (62, 63). In
518 agreement with Overduin's interpretations, it seems likely that the motor cortex may function to
519 combine brainstem or spinal synergies (via polysynaptic innervation) with control of individual muscles
520 that are responsible for individuated, dexterous, hand movement (24, 25).
521
522 However, we cannot rule out the possibility that the TMS-elicited synergies may be cortical in
523 origin, for example via either the divergence of corticomotor neurons or via intracortical horizontal
524 connections between corticomotor neurons. Retrograde viral tracing (64, 65) as well as stimulus-
525 triggered averaging of EMG activity to ICSM have identified direct linkages from corticomotor neurons (66,
526 67) to the corticomotor neuron pools of multiple muscles. Synergistic patterns of voluntary muscle
527 activation likely result from modularity inherent in organization at the cortical, brain stem, and spinal
528 level (68). Future research, perhaps utilizing TMS to stimulate the brain stem and spine, may help
529 elucidate the contribution of each structure to modularity in voluntary control.
530
531 **4.3. Similarity of Synergies across Individuals**
532

533 A group-level analysis revealed that individual synergies showed greater than chance similarity
534 across subjects for TMS and voluntary data. This finding was corroborated by the results of the cluster
535 analysis which showed that 54/80 (27/40 per condition) synergies (cluster 1-4) were nearly equally
536 distributed across TMS and VOL data sets. The observed inter-individual similarity is in general
537 agreement with that reported for healthy individuals by Roh et. al. (15, 50) who described inter-
538 individual similarity of synergies, using similar methodology to ours, extracted from upper limb muscles
539 during a force production task. While it is possible that the inter-individual similarity in voluntary
540 synergies may be attributed to the constraints of the finger spelling task used in our study (19), task-
541 dependence is unlikely to underlie the inter-individual similarity of TMS-elicited synergies. A plausible
542 explanation for the latter can be drawn from the work of Ejaz et. al. (69), who used fMRI to show that
543 the correlational structure amongst digit topographies may be dictated by the statistics of everyday
544 hand use. They suggested that the strength of horizontal intracortical connections within M1 may be
545 determined by the frequency with which those connections are activated, in a Hebbian type manner,
546 and reason that activation of these connections could explain the results of Overduin et. al. (25). All
547 participants enrolled in our study were naive to the ASL alphabet, and the task of finger spelling in
548 general. Given the reasonable assumption that our participants had fairly similar statistics of everyday
549 hand use over the course of their lives (participants did not report any specific digit training such as
550 musical training), we contend that the hypotheses offered by Ejaz et. al. (69) best explain the inter-
551 individual similarity observed in the TMS-elicited synergies.
552
553 Furthermore, it has previously been shown that short periods of training can elicit
554 reorganization of the cortical representation for simple finger movements revealed by TMS (54). Two
555 more recent studies have extended these findings to more complex movements of the hand using
556 TMS evoked postural synergies to demonstrate that highly specific motor training can induce short-
557 term modulation of a selected set of synergies associated with the training activity (70, 71). We
558 purposely conducted TMS mapping prior to performance of the ASL task to avoid such recency bias
559 influencing TMS results. However, whether synergies extracted from TMS responses were influenced

by recently practiced movements by our participants outside of the laboratory is unknown. To what extent TMS-evoked muscle synergies, as described in our study, represent recent motor learning, long term motor practice (28), or the natural statistics of hand use over the lifetime (69, 72) remains an open and interesting question. Future research using the technique suggested here could offer valuable insight into whether the structure of TMS-elicited muscle synergies does indeed reflect short- or long-term encoding of skill (such as differences between novice learners and experts in ASL).

4.4 Potential limitations and future directions

Several recent reports have highlighted that the structure and interpretation of muscle synergies may be influenced by EMG filtering parameters, method of EMG amplitude normalization, and the selection of the dimensionality reduction algorithm (47, 73-75). Given that synergy extraction from MEPs is highly novel, future studies should examine the influence of preprocessing steps and dimensionality reduction techniques on the structure and interpretability of synergies derived from M1 TMS.

The composition of synergies is dependent upon number and choice of muscles analyzed (76). In our study, we measured eight muscles (of more than 30 that comprise the hand/wrist musculature) and our results may only extend to these 8 muscles. As suggested in (76), we selected a "dominant" set of muscles with the goal of including primary intrinsic and extrinsic muscles that would be strongly recruited in the finger spelling task, while still being able to maximize the distance between the electrodes in order to minimize cross-talk—which could have potentially confounded our experiment. We also only included muscles for which measurement was possible with surface EMG. Certainly the inclusion of more (or less) muscles may influence findings about the similarity of TMS-induced and voluntary muscle synergies.

586 As has been done by others (15), we chose to extract an equal number of synergies from each
587 dataset to facilitate comparisons of synergies across tasks and individuals. That 5 synergies provided
588 a valid characterization of modularity in muscle activation across tasks and individuals was justified by
589 the high overall and muscle specific reconstruction accuracy using 5 synergies, and the lack of large
590 differences (<5% R^2) found between 4 and 5, or 5 and 6 synergies for any one dataset. However, a
591 greater number of synergies was more often required to satisfy the 90% R^2 criterion in the voluntary
592 data (Fig. 4). Possible greater complexity of the voluntary data is unsurprising given the known
593 contributions of brain stem, spinal, and peripheral contributions to voluntary activation.
594
595 In an effort to utilize as many stimulations as possible, we retained stimulations with slight
596 background EMG activity prior to stimulation in the analyses (see Figure 3, ADM). Pre-activation of the
597 muscle will increase MEP amplitude (77), potentially increasing the weight of a specific trial or more
598 generally a muscle when subjected to NMF. Large MEPs resulting from pre-activation also pose a
599 possible threat to the validity of using the maximum MEP across trials for normalization. The similarity
600 we observed between TMS-elicited and voluntary muscle synergies was found in spite of this potential
601 confound, which is not present in the voluntary data set. Previous empirical evidence indicating
602 similarity between TMS-elicited and voluntary postural synergies of the hand also may have been
603 observed despite slight background EMG activity, as in that study only audio feedback of a single
604 muscle was used to ensure relaxation (27). Achieving complete relaxation in all muscles just prior to
605 TMS is a challenge of mapping hand postures or a large number of muscles simultaneously. Data
606 from a larger sample is needed to set guidelines for experimental procedures and data preprocessing
607 for synergy analysis of multi-muscle TMS, and multi-muscle TMS mapping more generally in order to
608 optimize data quality, reliability, and experimental efficiency.
609
610 Another potential limitation of the present study is the possibility of cross-talk between EMG
611 channels influencing the results of NMF. Consistent correlation between electrode recordings due to
612 cross-talk would potentially be reflected in the synergy bases given the implementation of NMF utilized

613 in the study (78). However, the results of two previous studies indicate that this is unlikely. Cross-talk
614 between electrodes was previously found to have minimal influence on the results of synergy analysis
615 performed on EMG data recorded from the legs of neonates (79). We propose that if synergy analysis
616 is not confounded by cross-talk between EMGs placed on the legs of neonates, it is unlikely to be a
617 factor in the collection of muscles from an adult arm/hand. Furthermore, in a study of human
618 locomotion, whether synergies (computed using PCA) were derived from the surface or intramuscular
619 EMG did not significantly influence the resulting principal components indicating the influence of cross-
620 talk derived synergies was minimal (78).

621 Only a single task, finger spelling, was used to assess voluntary synergies. It has been
622 suggested that synergies may be an artifact of the movement variance in the task from which they were
623 collected (19). Although we cannot rule out the possibility that the voluntary synergies were task-
624 dependent, similar work in our lab has shown that synergies derived from unconstrained (task-free)
625 movement can be used for the prediction of synergies extracted from ASL postures as well as those
626 extracted from grasping mimicking postures with an accuracy that is nearly equal to prediction from
627 synergies derived from task specific muscle activation (80). Critically, the synergies derived at rest from
628 the TMS data set clearly are not confounded by task. Although the task-dependence of synergies is an
629 interesting question that requires further investigation, we do not think that this confounds the findings
630 of our study.

631

632 TMS-elicited and voluntary EMG were collected in a single upper limb posture, therefore we
633 are not able to comment on the effects of limb posture on the observed modularity. Though a recent
634 investigation indicated that the overall muscles synergy structure was largely unaffected by changes in
635 shoulder posture during a shoulder torque production task (81), the effects upperlimb posture on the
636 specific task utilized in this study are unknown and may be worthy of future investigation.

637

638 EMG only from the static "hold" portion of the ASL task was used in synergy analysis of
639 voluntary movement. This choice was made in order to yield a more direct comparison to the findings of

Gentner and Classen (27) where a single hand posture was used to describe TMS-elicited movements. The extent to which TMS-elcited muscle synergies reflect voluntary muscle synergies de- rived during dynamic movement remains an open question.

We tested at a single stimulation intensity (110% RMT); it would be very interesting and relevant to carry out this protocol at multiple suprathreshold intensities. As discussed above, the choice of stimulation intensity has a profound impact on corticospinal outputs. Likewise, pulse shape (monophasic/biphasic) and current direction (PA/AP) are known to have differential effects on corticospinal responses to TMS (82). In this study a biphasic stimulation waveform and PA current direction were used. It is unknown whether similarity between TMS and voluntary synergies observed here is specific to the coil parameters used. Assessment of the effect of stimulus intensity, pulse shape, and current direction on the structure of TMS-elicited muscle synergies is needed to better understand how TMS can be utilized to examine the neural substrates of motor modularity.

In contrast to the ”time-invariant” synergies described in this paper for which temporal aspects of muscle activation are relegated solely to the activation matrix, dimensionality reduction algorithms can also be used to compute ”time-varying” muscle synergies in which the spatiotemporal features of muscle activation are represented within the synergies (83). Analysis of time-varying synergies using TMS is not straightforward because the MEP is generally regarded as a temporally discrete event. A clever experimental design in which TMS was applied during movement or perhaps during motor imagery may yield interesting insights into modularity in EMG bursting patterns as described by time-varying synergies. For example, this technique could be used to test the hypothesis that patchy redundant cortical somatotopy representing static muscle synergies is optimally organized to produce fluid spatiotemporal sequences of hand movements proposed in a recent investigation of time-varying muscle synergies during finger spelling (84).

666 The scope of the current study was to understand the synergistic muscle activation patterns
667 evoked by TMS and voluntary movement. However, an equally interesting question, beyond the scope
668 of this study, is how individual muscles and synergies topographically map back on the cortical sheet.
669 To what degree will this organization be parcelled or intermingled? Previous attempts to do so using
670 TMS (27, 85-88) have relied on a highly reductionist approach, attributing the muscular or kinematic
671 response to a point on the scalp representing the site of neural activation induced by the TMS. These
672 studies have generally examined the degree of overlap between individual muscle "mappings" in
673 relation to the co-activation or co-variation of muscle responses. The work generally converges on the
674 finding that a high degree of overlap exists, and often there is a correspondence between the degree of
675 overlap and the co-variation of muscle responses. However, these approaches tend to be limited in
676 their ability to draw inferential conclusions about how topographic organization may be related to
677 modular control. In order to address this challenge, we are currently developing a framework that uses
678 a deep neural network model to map finite element simulation of transcranial magnetic stimulation
679 induced electric fields in motor cortex to recordings of multi-muscle activation (89). Use of this
680 framework has the potential to produce higher resolution imaging of cortical-muscle mappings, with
681 consideration of individual anatomy, allowing for more rigorous investigation and interpretation of the
682 topographic characteristics of muscles and synergies.
683
684 **Conclusions**
685
686 Our work provides evidence that TMS-elicited muscle synergies of the hand, measured at rest,
687 reflect those found in voluntary behavior involving finger fractionation. Our findings build on those of
688 Gentner and Classen (27) and Overduin et. al. (25), by offering a more accessible way of assessing
689 modularity using cortical stimulation in humans. With further research to determine the robustness of
690 our findings to different stimulation parameters and analytical procedures, the technique offered here
691 can be used to develop insights into the nature of corticospinal modularity in learning, and its

692 breakdown and recovery in pathologies such as stroke, in which muscle co-activation patterns are
693 known to be affected (15, 50, 90).
694
695 **Acknowledgements**
696
697 We would like to thank Emilio Bizzi, Robert Ajemian and Vincent Cheung for their helpful
698 suggestions in the completion of this work. This project was supported by National Institute of Health
699 grants F31 NS092268 (MY), R01NS085122 (ET), 2R01HD058301 (ET), P41 GM10354518 (DB), R01
700 DC009834 (DE), and National Science Foundation grants IIS-1149570 (DE), CNS-1544895 (DE),
701 CBET-1804550 (ET,DE,DB), CMMI-1935337 (ET,DE,MY).
702
703

References

1. **Tresch MC, Saltiel P, and Bizzi E**. The construction of movement by the spinal cord. *Nat Neurosci* 2: 162-167, 1999.
2. **Bernstein NA**. The co-ordination and regulation of movements. *Pergamon Press, Oxford* 1967.
3. **Tresch MC, and Jarc A**. The case for and against muscle synergies. *Curr Opin Neurobiol* 19: 601-607, 2009.
4. **Bizzi E, Cheung VC, d'Avella A, Saltiel P, and Tresch M**. Combining modules for movement. *Brain research reviews* 57: 125-133, 2008.
5. **Santello M, Flanders M, and Soechting JF**. Postural hand synergies for tool use. *The Journal of neuroscience : the official journal of the Society for Neuroscience* 18: 10105-10115, 1998.
6. **Cheung VCK, and Seki K**. Approaches to revealing the neural basis of muscle synergies: a review and a critique. *Journal of neurophysiology* 125: 1580-1597, 2021.
7. **Bizzi E, and Cheung VC**. The neural origin of muscle synergies. *Front Comput Neurosci* 7: 51, 2013.
8. **Alessandro C, Oliveira Barroso F, and Tresch M**. Working hard to make a simple definition of synergies: Comment on: "Hand synergies: Integration of robotics and neuroscience for understanding the control of biological and artificial hands" by Marco Santello et al. *Physics of life reviews* 17: 24-26, 2016.
9. **Giszter SF, Mussa-Ivaldi FA, and Bizzi E**. Convergent force fields organized in the frog's spinal cord. *The Journal of neuroscience : the official journal of the Society for Neuroscience* 13: 467-491, 1993.
10. **Ting LH, and Macpherson JM**. A limited set of muscle synergies for force control during a postural task. *Journal of neurophysiology* 93: 609-613, 2005.
11. **Mason CR, Theverapperuma LS, Hendrix CM, and Ebner TJ**. Monkey hand postural synergies during reach-to-grasp in the absence of vision of the hand and object. *Journal of neurophysiology* 91: 2826-2837, 2004.
12. **d'Avella A, Saltiel P, and Bizzi E**. Combinations of muscle synergies in the construction of a natural motor behavior. *Nat Neurosci* 6: 300-308, 2003.
13. **Ting LH, and McKay JL**. Neuromechanics of muscle synergies for posture and movement. *Curr Opin Neurobiol* 17: 622-628, 2007.
14. **Overduin SA, d'Avella A, Carmena JM, and Bizzi E**. Muscle synergies evoked by microstimulation are preferentially encoded during behavior. *Front Comput Neurosci* 8: 20, 2014.
15. **Roh J, Rymer WZ, Perreault EJ, Yoo SB, and Beer RF**. Alterations in upper limb muscle synergy structure in chronic stroke survivors. *Journal of neurophysiology* 109: 768-781, 2013.
16. **Cheung VC, Turolla A, Agostini M, Silvoni S, Bennis C, Kasi P, Paganoni S, Bonato P, and Bizzi E**. Muscle synergy patterns as physiological markers of motor cortical damage. *Proceedings of the National Academy of Sciences of the United States of America* 109: 14652-14656, 2012.
17. **Ajiboye AB, and Weir RF**. Muscle synergies as a predictive framework for the EMG patterns of new hand postures. *Journal of neural engineering* 6: 036004, 2009.
18. **Torres-Oviedo G, and Ting LH**. Muscle synergies characterizing human postural responses. *Journal of neurophysiology* 98: 2144-2156, 2007.
19. **Diedrichsen J, Shadmehr R, and Ivry RB**. The coordination of movement: optimal feedback control and beyond. *Trends in cognitive sciences* 14: 31-39, 2010.
20. **Kutch JJ, and Valero-Cuevas FJ**. Challenges and new approaches to proving the existence of muscle synergies of neural origin. *PLoS Comput Biol* 8: e1002434, 2012.
21. **Berger DJ, Gentner R, Edmunds T, Pai DK, and d'Avella A**. Differences in adaptation rates after virtual surgeries provide direct evidence for modularity. *The Journal of neuroscience : the official journal of the Society for Neuroscience* 33: 12384-12394, 2013.

22. **Takei T, Confais J, Tomatsu S, Oya T, and Seki K**. Neural basis for hand muscle synergies in the primate spinal cord. *Proceedings of the National Academy of Sciences of the United States of America* 114: 8643-8648, 2017.
23. **Graziano MS, Taylor CS, and Moore T**. Complex movements evoked by microstimulation of precentral cortex. *Neuron* 34: 841-851, 2002.
24. **Overduin SA, d'Avella A, Roh J, and Bizzi E**. Modulation of muscle synergy recruitment in primate grasping. *The Journal of neuroscience : the official journal of the Society for Neuroscience* 28: 880-892, 2008.
25. **Overduin SA, d'Avella A, Carmena JM, and Bizzi E**. Microstimulation activates a handful of muscle synergies. *Neuron* 76: 1071-1077, 2012.
26. **Amundsen Huffmaster SL, Van Acker GM, 3rd, Luchies CW, and Cheney PD**. Muscle synergies obtained from comprehensive mapping of the primary motor cortex forelimb representation using high-frequency, long-duration ICMS. *Journal of neurophysiology* 118: 455-470, 2017.
27. **Gentner R, and Classen J**. Modular organization of finger movements by the human central nervous system. *Neuron* 52: 731-742, 2006.
28. **Gentner R, Gorges S, Weise D, aufm Kampe K, Buttmann M, and Classen J**. Encoding of motor skill in the corticomuscular system of musicians. *Current biology : CB* 20: 1869-1874, 2010.
29. **Di Lazzaro V, Oliviero A, Profice P, Ferrara L, Saturno E, Pilato F, and Tonali P**. The diagnostic value of motor evoked potentials. *Clinical neurophysiology : official journal of the International Federation of Clinical Neurophysiology* 110: 1297-1307, 1999.
30. **Yarossi M, Patel J, Qiu Q, Massood S, Fluet G, Merians A, Adamovich S, and Tunik E**. The Association Between Reorganization of Bilateral M1 Topography and Function in Response to Early Intensive Hand Focused Upper Limb Rehabilitation Following Stroke Is Dependent on Ipsilesional Corticospinal Tract Integrity. *Frontiers in neurology* 10: 258, 2019.
31. **Smith MC, Ackerley SJ, Barber PA, Byblow WD, and Stinear CM**. PREP2 Algorithm Predictions Are Correct at 2 Years Poststroke for Most Patients. *Neurorehabilitation and neural repair* 33: 635-642, 2019.
32. **Oldfield RC**. The assessment and analysis of handedness: the Edinburgh inventory. *Neuropsychologia* 9: 97-113, 1971.
33. **Keel JC, Smith MJ, and Wassermann EM**. A safety screening questionnaire for transcranial magnetic stimulation. *Clinical neurophysiology : official journal of the International Federation of Clinical Neurophysiology* 112: 720, 2001.
34. **Littmann AE, McHenry CL, and Shields RK**. Variability of motor cortical excitability using a novel mapping procedure. *Journal of neuroscience methods* 214: 137-143, 2013.
35. **Conforto AB, Z'Graggen WJ, Kohl AS, Rosler KM, and Kaelin-Lang A**. Impact of coil position and electrophysiological monitoring on determination of motor thresholds to transcranial magnetic stimulation. *Clinical neurophysiology : official journal of the International Federation of Clinical Neurophysiology* 115: 812-819, 2004.
36. **Koski L, Mernar TJ, and Dobkin BH**. Immediate and long-term changes in corticomotor output in response to rehabilitation: correlation with functional improvements in chronic stroke. *Neurorehabilitation and neural repair* 18: 230-249, 2004.
37. **Sparing R, Buelte D, Meister IG, Paus T, and Fink GR**. Transcranial magnetic stimulation and the challenge of coil placement: a comparison of conventional and stereotaxic neuronavigational strategies. *Human brain mapping* 29: 82-96, 2008.
38. **Niskanen E, Julkunen P, Saisanen L, Vanninen R, Karjalainen P, and Kononen M**. Group-level variations in motor representation areas of thenar and anterior tibial muscles: Navigated Transcranial Magnetic Stimulation Study. *Human brain mapping* 31: 1272-1280, 2010.
39. **Yarossi M, Adamovich S, and Tunik E**. Sensorimotor cortex reorganization in subacute and chronic stroke: A neuronavigated TMS study. *Annual International Conference of the IEEE Engineering*

in Medicine and Biology Society IEEE Engineering in Medicine and Biology Society Annual International Conference 2014: 5788-5791, 2014.

40. **Faghihpirayesh R, Imbiriba T, Yarossi M, Tunik E, Brooks D, and Erdogmus D**. Motor Cortex Mapping using Active Gaussian Processes. *The International Conference on PErvasive Technologies Related to Assistive Environments : PETRA International Conference on PErvasive Technologies Related to Assistive Environments* 2020: 2020.

41. **Jonker ZD, van der Vliet R, Hauwert CM, Gaiser C, Tulen JHM, van der Geest JN, Donchin O, Ribbers GM, Frens MA, and Selles RW**. TMS motor mapping: Comparing the absolute reliability of digital reconstruction methods to the golden standard. *Brain stimulation* 12: 309-313, 2019.

42. **van de Ruit M, Perenboom MJ, and Grey MJ**. TMS brain mapping in less than two minutes. *Brain stimulation* 8: 231-239, 2015.

43. **Lee DD, and Seung HS**. Learning the parts of objects by non-negative matrix factorization. *Nature* 401: 788-791, 1999.

44. **Cheung VC, d'Avella A, Tresch MC, and Bizzi E**. Central and sensory contributions to the activation and organization of muscle synergies during natural motor behaviors. *The Journal of neuroscience : the official journal of the Society for Neuroscience* 25: 6419-6434, 2005.

45. **Tresch MC, Cheung VC, and d'Avella A**. Matrix factorization algorithms for the identification of muscle synergies: evaluation on simulated and experimental data sets. *Journal of neurophysiology* 95: 2199-2212, 2006.

46. **Lambert-Shirzad N, and Van der Loos HF**. On identifying kinematic and muscle synergies: a comparison of matrix factorization methods using experimental data from the healthy population. *Journal of neurophysiology* 117: 290-302, 2017.

47. **Turpin NA, Uriac S, and Dalleau G**. How to improve the muscle synergy analysis methodology? *European journal of applied physiology* 121: 1009-1025, 2021.

48. **Devarajan K, and Cheung VC**. On nonnegative matrix factorization algorithms for signal-dependent noise with application to electromyography data. *Neural computation* 26: 1128-1168, 2014.

49. **d'Avella A, Portone A, Fernandez L, and Lacquaniti F**. Control of fast-reaching movements by muscle synergy combinations. *The Journal of neuroscience : the official journal of the Society for Neuroscience* 26: 7791-7810, 2006.

50. **Roh J, Rymer WZ, and Beer RF**. Evidence for altered upper extremity muscle synergies in chronic stroke survivors with mild and moderate impairment. *Frontiers in human neuroscience* 9: 6, 2015.

51. **Weiss EJ, and Flanders M**. Muscular and postural synergies of the human hand. *Journal of neurophysiology* 92: 523-535, 2004.

52. **Tagliabue M, Ciancio AL, Brochier T, Eskiizmirliler S, and Maier MA**. Differences between kinematic synergies and muscle synergies during two-digit grasping. *Frontiers in human neuroscience* 9: 165, 2015.

53. **Lang CE, and Schieber MH**. Reduced muscle selectivity during individuated finger movements in humans after damage to the motor cortex or corticospinal tract. *Journal of neurophysiology* 91: 1722-1733, 2004.

54. **Classen J, Liepert J, Wise SP, Hallett M, and Cohen LG**. Rapid plasticity of human cortical movement representation induced by practice. *Journal of neurophysiology* 79: 1117-1123, 1998.

55. **Franza M, Sorrentino G, Vissani M, Serino A, Blanke O, and Bassolino M**. Hand perceptions induced by single pulse transcranial magnetic stimulation over the primary motor cortex. *Brain stimulation* 12: 693-701, 2019.

56. **Rothwell JC**. Techniques and mechanisms of action of transcranial stimulation of the human motor cortex. *Journal of neuroscience methods* 74: 113-122, 1997.

57. **Di Lazzaro V, Oliviero A, Profice P, Saturno E, Pilato F, Insola A, Mazzone P, Tonali P, and Rothwell JC**. Comparison of descending volleys evoked by transcranial magnetic and electric

stimulation in conscious humans. *Electroencephalography and clinical neurophysiology* 109: 397-401, 1998.

58. **Di Lazzaro V, Profice P, Ranieri F, Capone F, Dileone M, Oliviero A, and Pilato F**. I-wave origin and modulation. *Brain stimulation* 5: 512-525, 2012.

59. **Zaaimi B, Dean LR, and Baker SN**. Different contributions of primary motor cortex, reticular formation, and spinal cord to fractionated muscle activation. *Journal of neurophysiology* 119: 235-250, 2018.

60. **Lawrence DG, and Kuypers HG**. The functional organization of the motor system in the monkey. I. The effects of bilateral pyramidal lesions. *Brain : a journal of neurology* 91: 1-14, 1968.

61. **Porter R, and Lemon R**. *Corticospinal function and voluntary movement*. USA: Oxford University Press, 1993.

62. **Hart CB, and Giszter SF**. A neural basis for motor primitives in the spinal cord. *The Journal of neuroscience : the official journal of the Society for Neuroscience* 30: 1322-1336, 2010.

63. **Roh J, Cheung VC, and Bizzi E**. Modules in the brain stem and spinal cord underlying motor behaviors. *Journal of neurophysiology* 106: 1363-1378, 2011.

64. **Rathelot JA, and Strick PL**. Subdivisions of primary motor cortex based on cortico-motoneuronal cells. *Proceedings of the National Academy of Sciences of the United States of America* 106: 918-923, 2009.

65. **Rathelot JA, and Strick PL**. Muscle representation in the macaque motor cortex: an anatomical perspective. *Proceedings of the National Academy of Sciences of the United States of America* 103: 8257-8262, 2006.

66. **Park MC, Belhaj-Saif A, and Cheney PD**. Properties of primary motor cortex output to forelimb muscles in rhesus macaques. *Journal of neurophysiology* 92: 2968-2984, 2004.

67. **Griffin DM, Hudson HM, Belhaj-Saif A, and Cheney PD**. EMG activation patterns associated with high frequency, long-duration intracortical microstimulation of primary motor cortex. *The Journal of neuroscience : the official journal of the Society for Neuroscience* 34: 1647-1656, 2014.

68. **McMorland AJ, Runnalls KD, and Byblow WD**. A neuroanatomical framework for upper limb synergies after stroke. *Frontiers in human neuroscience* 9: 82, 2015.

69. **Ejaz N, Hamada M, and Diedrichsen J**. Hand use predicts the structure of representations in sensorimotor cortex. *Nat Neurosci* 18: 1034-1040, 2015.

70. **Hirano M, Kubota S, Furuya S, Koizume Y, Tanaka S, and Funase K**. Acquisition of skilled finger movements is accompanied by reorganization of the corticospinal system. *Journal of neurophysiology* 119: 573-584, 2018.

71. **Fricke C, Gentner R, Alizadeh J, and Classen J**. Linking Individual Movements to a Skilled Repertoire: Fast Modulation of Motor Synergies by Repetition of Stereotyped Movements. *Cerebral cortex* 30: 1185-1198, 2020.

72. **Leo A, Handjaras G, Bianchi M, Marino H, Gabiccini M, Guidi A, Scilingo EP, Pietrini P, Bicchi A, Santello M, and Ricciardi E**. A synergy-based hand control is encoded in human motor cortical areas. *eLife* 5: 2016.

73. **Banks CL, Pai MM, McGuirk TE, Fregly BJ, and Patten C**. Methodological Choices in Muscle Synergy Analysis Impact Differentiation of Physiological Characteristics Following Stroke. *Front Comput Neurosci* 11: 78, 2017.

74. **Kieliba P, Tropea P, Pirondini E, Coscia M, Micera S, and Artoni F**. How are Muscle Synergies Affected by Electromyography Pre-Processing? *IEEE transactions on neural systems and rehabilitation engineering : a publication of the IEEE Engineering in Medicine and Biology Society* 26: 882-893, 2018.

75. **Shuman BR, Schwartz MH, and Steele KM**. Electromyography Data Processing Impacts Muscle Synergies during Gait for Unimpaired Children and Children with Cerebral Palsy. *Front Comput Neurosci* 11: 50, 2017.

76. **Steele KM, Tresch MC, and Perreault EJ**. The number and choice of muscles impact the results of muscle synergy analyses. *Front Comput Neurosci* 7: 105, 2013.
77. **Hallett M**. Transcranial magnetic stimulation: a primer. *Neuron* 55: 187-199, 2007.
78. **Hug F, Turpin NA, Guevel A, and Dorel S**. Is interindividual variability of EMG patterns in trained cyclists related to different muscle synergies? *Journal of applied physiology* 108: 1727-1736, 2010.
79. **Dominici N, Ivanenko YP, Cappellini G, d'Avella A, Mondi V, Cicchese M, Fabiano A, Silei T, Di Paolo A, Giannini C, Poppele RE, and Lacquaniti F**. Locomotor primitives in newborn babies and their development. *Science* 334: 997-999, 2011.
80. **Gunay SY, Yarossi M, Brooks DH, Tunik E, and Erdogmus D**. Transfer learning using low-dimensional subspaces for EMG-based classification of hand posture. *International IEEE/EMBS Conference on Neural Engineering : [proceedings] International IEEE EMBS Conference on Neural Engineering* 2019: 1097-1100, 2019.
81. **Leonardis JM, Alkayyali AA, and Lipps DB**. Posture-dependent neuromuscular contributions to three-dimensional isometric shoulder torque generation. *Journal of neurophysiology* 123: 1526-1535, 2020.
82. **Sommer M, Alfaro A, Rummel M, Speck S, Lang N, Tings T, and Paulus W**. Half sine, monophasic and biphasic transcranial magnetic stimulation of the human motor cortex. *Clinical neurophysiology : official journal of the International Federation of Clinical Neurophysiology* 117: 838-844, 2006.
83. **d'Avella A, and Bizzi E**. Shared and specific muscle synergies in natural motor behaviors. *Proceedings of the National Academy of Sciences of the United States of America* 102: 3076-3081, 2005.
84. **Klein Breteler MD, Simura KJ, and Flanders M**. Timing of muscle activation in a hand movement sequence. *Cerebral cortex* 17: 803-815, 2007.
85. **Devanne H, Cassim F, Ethier C, Brizzi L, Thevenon A, and Capaday C**. The comparable size and overlapping nature of upper limb distal and proximal muscle representations in the human motor cortex. *The European journal of neuroscience* 23: 2467-2476, 2006.
86. **Masse-Alarie H, Bergin MJG, Schneider C, Schabrun S, and Hodges PW**. "Discrete peaks" of excitability and map overlap reveal task-specific organization of primary motor cortex for control of human forearm muscles. *Human brain mapping* 38: 6118-6132, 2017.
87. **Melgari JM, Pasqualetti P, Pauri F, and Rossini PM**. Muscles in "concert": study of primary motor cortex upper limb functional topography. *PloS one* 3: e3069, 2008.
88. **Mathew J, Kubler A, Bauer R, and Gharabaghi A**. Probing Corticospinal Recruitment Patterns and Functional Synergies with Transcranial Magnetic Stimulation. *Frontiers in cellular neuroscience* 10: 175, 2016.
89. **Yarossi M, Quivira F, Dannhauer M, Sommer MA, Brooks DH, Erdogmus D, and Tunik E**. An experimental and computational framework for modeling multi-muscle responses to transcranial magnetic stimulation of the human motor cortex. *International IEEE/EMBS Conference on Neural Engineering : [proceedings] International IEEE EMBS Conference on Neural Engineering* 2019: 1122-1125, 2019.
90. **Cheung VC, Piron L, Agostini M, Silvoni S, Turolla A, and Bizzi E**. Stability of muscle synergies for voluntary actions after cortical stroke in humans. *Proceedings of the National Academy of Sciences of the United States of America* 106: 19563-19568, 2009.

946 Table 1. *Comparison of Reconstruction and Cross-Reconstruction for within and across muscles using*
947 *repeated measures ANOVAs with factors of Data Source (TMS, VOL) and Reconstruction Type (Within*
948 *R^2, Cross R^2_{CR}). Significant outcomes are highlighted in bold text.*

Muscle	Data Source	Reconstruction Type	Interactions	Posthocs
FDI	***F(1,7)* = 9.89, *P* = 0.016**	***F(1,7)* = 13.02 , *P* = 0.009**	***F(1,7)* = 9.26, *P* = 0.019**	TMS vs. TMScr: *t(7)* = 0.704, *P* = 0.504 **VOL vs VOLcr: *t(7)* = 3.43, *P* = 0.011** TMS vs VOL: *t(7)* = –0.827, *P* = 0.436 TMScr vs. VOLcr: *t(7)* = 3.154, *P* = 0.016
EI	*F(1,7)* = 3.85, *P* = 0.091	***F(1,7)* = 22.63, *P* = 0.002**	*F(1,7)* = 0.80 , *P* = 0.401	**TMS vs. TMScr: *t(7)* = 4.221, *P* = 0.004** VOL vs VOLcr: *t(7)* = 2.371, *P* = 0.050 TMS vs VOL: *t(7)* = 2.779, *P* = 0.027 TMScr vs. VOLcr: *t(7)* = 0.445, *P* = 0.669
APB	*F(1,7)* = 2.742 , *P* = 0.142	***F(1,7)* = 8.47, *P* = 0.023**	*F(1,7)* = 0.674 , *P* = 0.439	TMS vs. TMScr: *t(7)* = 0.448, *P* = 0.641 VOL vs VOLcr: *t(7)* = 1.520, *P* = 0.172 TMS vs VOL: *t(7)* = –0.066, *P* = 0.949 TMScr vs. VOLcr: *t(7)* = 1.248, *P* = 0.252
ADM	*F(1,7)* = 1.947, *P* = 0.206	***F(1,7)* = 9.091, *P* = 0.020**	*F(1,7)* = 3.002, *P* = 0.127	TMS vs. TMScr: *t(7)* = 0.985, *P* = 0.358 VOL vs VOLcr: *t(7)* = 2.908, *P* = 0.023 TMS vs VOL: *t(7)* = –1.348, *P* = 0.220 TMScr vs. VOLcr: *t(7)* = 1.652, *P* = 0.143
FDS	*F(1,7)* = 0.943, *P* = 0.364	***F(1,7)* = 13.365, *P* = 0.008**	*F(1,7)* = .028, *P* = 0.871	TMS vs. TMScr: *t(7)* = 2.819, *P* = 0.026 VOL vs VOLcr: *t(7)* = 2.411, *P* = 0.047 TMS vs VOL: *t(7)* = 0.910, *P* = 0.393 TMScr vs. VOLcr: *t(7)* = 0.580, *P* = 0.580
EDC	*F(1,7)* = 0.311, *P* = 0.594	***F(1,7)* = 7.718, *P* = 0.027**	*F(1,7)* = 0.047, *P* = 0.835	TMS vs. TMScr: *t(7)* = 2.290, *P* = 0.056 VOL vs VOLcr: *t(7)* = 2.067, *P* = 0.078 TMS vs VOL: *t(7)* = 0.911, *P* = 0.392 TMScr vs. VOLcr: *t(7)* = 0.184, *P* = 0.859
FCR	*F(1,7)* = 1.094, *P* = 0.330	***F(1,7)* = 25.110, *P* = 0.002**	*F(1,7)* = 0.278, *P* = 0.614	TMS vs. TMScr: *t(7)* = 2.862, *P* = 0.024 **VOL vs VOLcr: *t(7)* = 3.732, *P* = 0.007** TMS vs VOL: *t(7)* = 0.413, *P* = 0.692 TMScr vs. VOLcr: *t(7)* = 0.837, *P* = 0.430
ECR	*F(1,7)* = 1.826, *P* = 0.219	***F(1,7)* = 12.770, *P* = 0.009**	*F(1,7)* = 0.041, *P* = 0.846	TMS vs. TMScr: *t(7)* = 1.855, *P* = 0.106 VOL vs VOLcr: *t(7)* = 1.475, *P* = 0.118 TMS vs VOL: *t(7)* = 1.306, *P* = 0.233 TMScr vs. VOLcr: *t(7)* = 0.677, *P* = 0.520
Global	***F(1,7)* = 9.948, *P* = 0.016**	***F(1,7)* = 138.798 , *P* < 0.001**	*F(1,7)* = 3.976, *P* = 0.086	**TMS vs. TMScr: *t(7)* = 8.782, *P* < 0.001** **VOL vs VOLcr: *t(7)* = 9.542, *P* < 0.001** **TMS vs VOL: *t(7)* = 3.680, *P* = 0.008** TMScr vs. VOLcr: *t(7)* = 2.745, *P* = 0.029

Fig. 1. Experimental design. Synergies were extracted from measurements of the same eight muscles using two different experimental approaches. On the left, TMS stimulation to locations on the motor cortex (red, yellow, and blue markers indicate three such sites) were used to acquire MEPs (shaded window) from eight wrist/hand muscles, shown as corresponding sets of 8 traces. On the right we show EMG acquired during the voluntary production of 3 hand postures in the ASL alphabet. The shaded regions indicate the window used for analysis. Muscle synergies were extracted using non-negative matrix factorization (NMF) for TMS and ASL data, and compared to investigate whether TMS-induced muscle synergies are consistent with those derived from voluntary hand movements. Data contained in this graphic is provided only to depict the experimental design and is not meant for interpretation.

959

960 Fig. 2. Visualization of the muscles of the right forearm/hand from which EMG activity was recorded in

961 the experiment.

962

963 Fig. 3. Raw data for used for synergy extraction for a representative participant. *A*: All MEPs recorded
964 during TMS mapping. A black vertical line indicates the time at which TMS was delivered. Grey shading
965 indicates the region in peak-to-peak amplitude of the MEP was calculated. *B*: Rectified EMGs recorded for a
966 single trial of the ASL task. Hand gestures for each sign are depicted in top left corner of each plot. Grey
967 shading indicates the region used for calculation of the root meansquare used for synergy extraction.

968

969 Fig. 4. Group average reconstruction R^2 by number of synergies for TMS (black) and Voluntary (grey)
970 datasets. As was expected, the R^2 curve for the shuffled data (dashed lines) increased approximately
971 linearly with increase rank of the synergy matrix *A*: Error bars indicate standard deviation. *B*: Number of
972 synergies chosen: Five muscle synergies were most commonly required to reconstruct 90% of the variance
973 in muscle activation patterns from TMS induced MEPs and voluntary EMG during the ASL task.

Fig. 5. Top. Reconstruction (black-dash) and cross-reconstruction (grey-dot) of TMS (left) and voluntary (right) data for a single participant. Muscle specific R^2 and R^2_{CR} values are displayed in black and grey respectively to the right of each plot. Bottom. Group average R^2 (black) and R^2_{CR} (grey) for each muscle and all muscles as a set (global, rightmost bars on each plot), again with TMS on the left and voluntary on the right. Note that vertical axes are labeled as variance explained (VE) to encompass both R^2 and R^2_{CR}. Chance estimates of R^2 and R^2_{CR}, derived from random shuffling of muscle identities in the synergy bases, are displayed in red. Reconstructions that were significantly different than chance ($P < 0.05$) are indicated with an asterisk.

983

984 Fig. 6. Cross-validated global reconstruction (R^2 & R^2_{CR}) for the reconstruction of voluntary EMG
985 during formation of ASL postures (Left) and MEPs recorded during TMS mapping of M1 (Right) for
986 each participant. Black bars indicate the cross-validated global reconstruction R^2 found from
987 reconstructing data using synergies derived from the same condition, and grey bars indicate the cross-
988 validated global cross-reconstruction R^2_{CR} found from reconstructing data using synergies derived from
989 the other condition. An independent sample *t*-test was used to test for differences between cross-
990 validated global reconstruction R^2 and cross-validated global cross-reconstruction R^2_{CR} for each
991 participant. Significantly lower reconstruction values (*, $P < 0.05$) when cross-fitting synergies from
992 one condition to the other (i.e., TMS to VOL) implies different synergy structure between the two
993 conditions. This finding is in agreement with group-level reconstruction and cross-reconstruction
994 results when the entire data set was used.

995

996 Fig. 7. Best-matching pairs of TMS-elicited synergies (black) and voluntary synergies (gray) for all individual
997 subjects. Synergy pairs for each individual are sorted from left to right based on the magnitude of the dot
998 product (number above each bar plot). Asterisks indicate dot-products that were significantly different from
999 the chance distribution (depicted to the right of matched pairs for each participant) determined by
1000 randomly shuffling the muscle identities (1,000 times per synergy) of TMS and VOL synergies and
1001 computing all possible dot products between shuffled synergies. The vertical red line indicates the 95th
1002 percentile of the chance distribution used as a threshold for significance and vertical black lines indicate
1003 the dot products of real matched pairs (values shown above each pair in the bar plots).

1004

1005 Fig. 8. *A*: Group mean synergies derived from TMS (left) and voluntary data. Synergies were sorted within
1006 each dataset using one subject selected at random, as a template synergy. Individual subject muscle
1007 synergy coefficients are represented with narrow bars, and the sample means for each muscle are
1008 represented by wide transparent bars with thick black outlines and error bars (± 1*STD*). Numbers just below
1009 each synergy label report the average dot product along with standard deviation between individual subject
1010 muscle coefficients and their respective group mean muscle coefficients for that synergy. Synergies are
1011 sorted top to bottom by the magnitude of the dot product between group average TMS and Voluntary
1012 synergies. *B*: Group average synergies, TMS in black and Voluntary in grey, are displayed back to back for
1013 ease of comparison. The dot product of each matched pair was significantly different (> 95th percentile)
1014 from a chance distribution determined by randomly shuffling the muscle identities (1,000 times per
1015 synergy) of group mean TMS and VOL synergies and computing all possible dot products between
1016 shuffled synergies.

1017

1018 Fig. 9. *A*: Composition, and *B*: Incidence of muscle synergy clusters. Five synergies were identified from

1019 each dataset (TMS,VOL) and clustered into nine groups (C1-C9).

1020

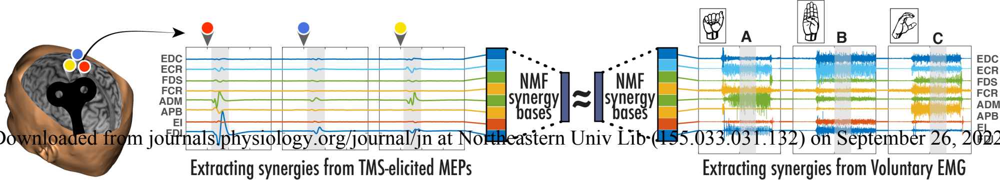
EDC
ECR
FDS
FCR
ADM
APB
EI
FDI
NMF synergy bases
≈
NMF synergy bases
A
B
C
EDC
ECR
FDS
FCR
ADM
APB
EI
FDI
Extracting synergies from TMS-elicited MEPs
Extracting synergies from Voluntary EMG

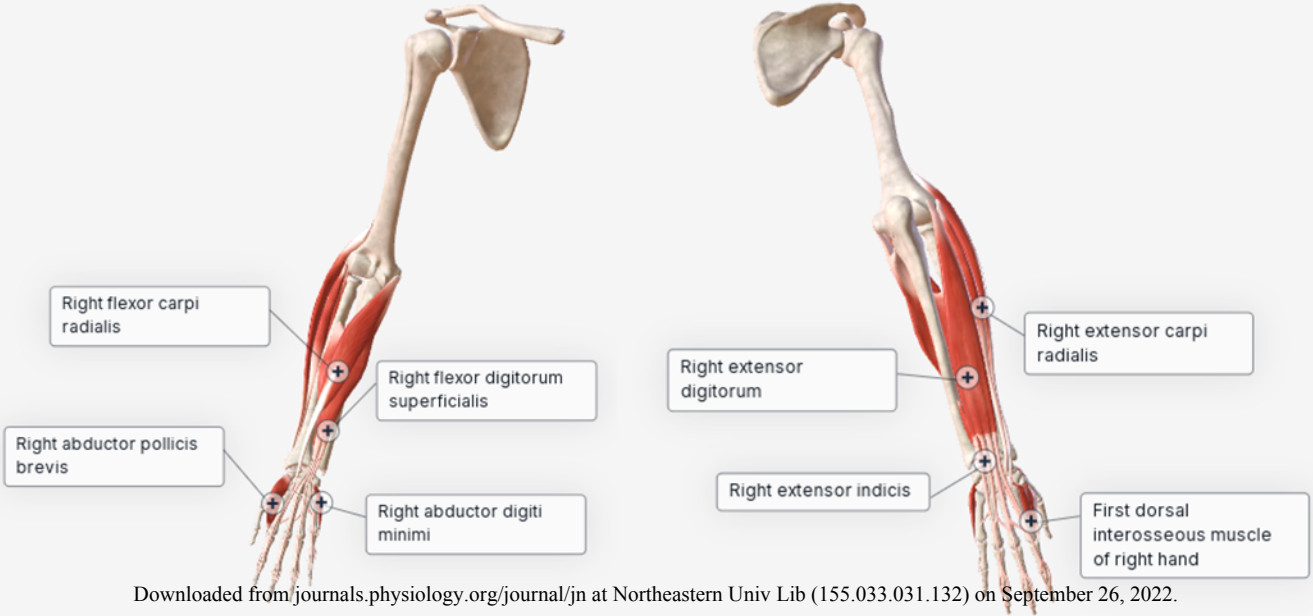

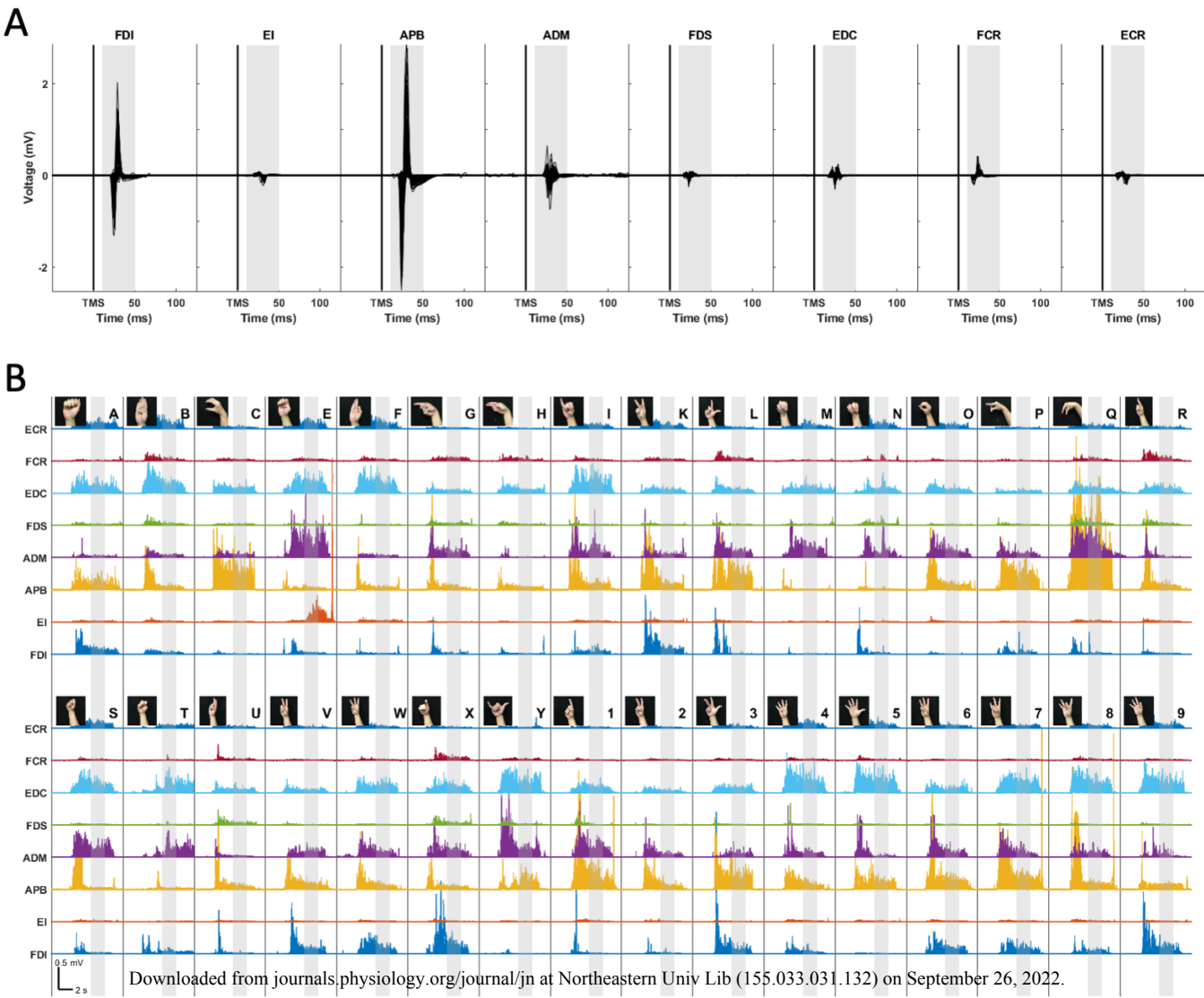

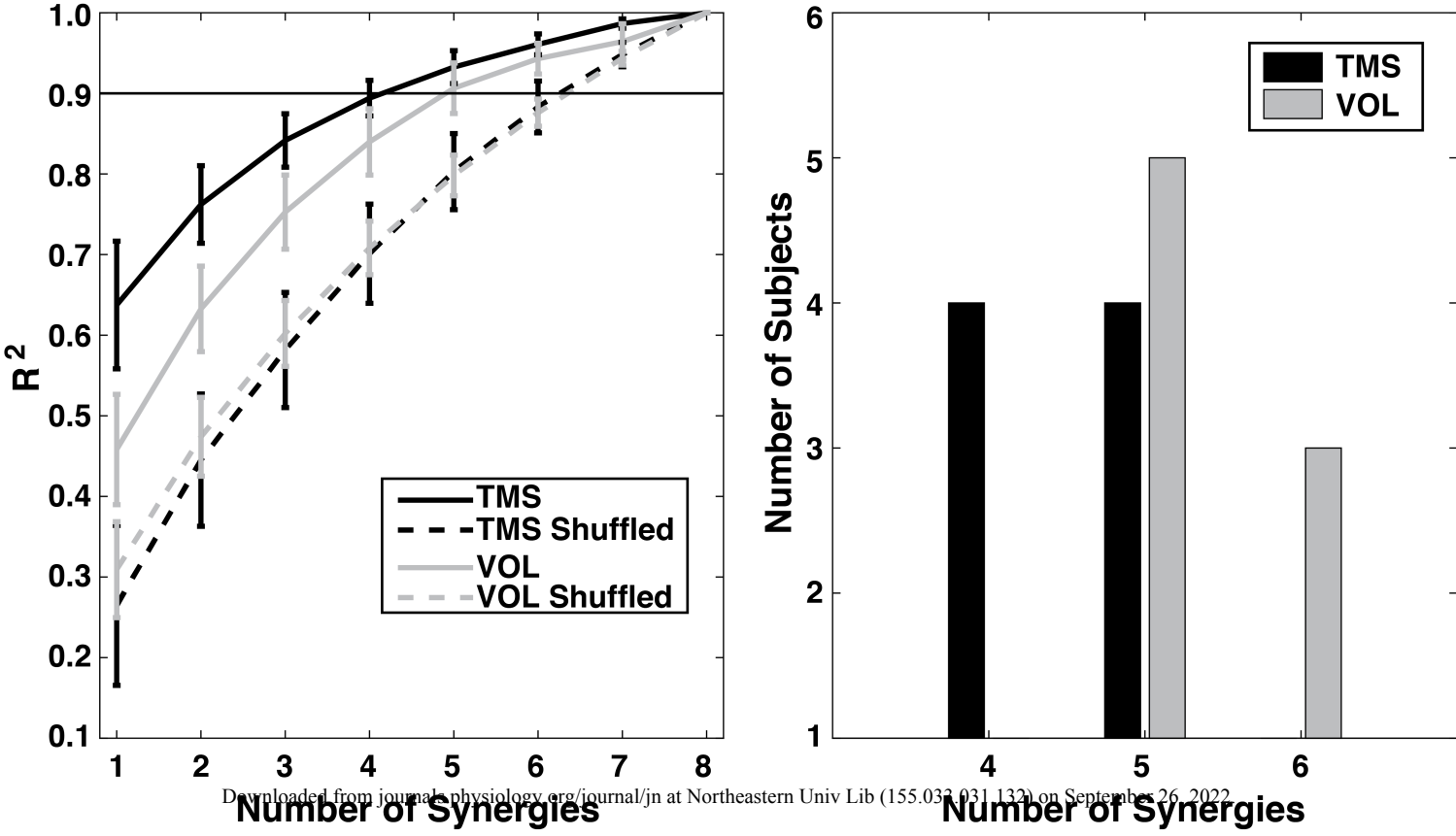

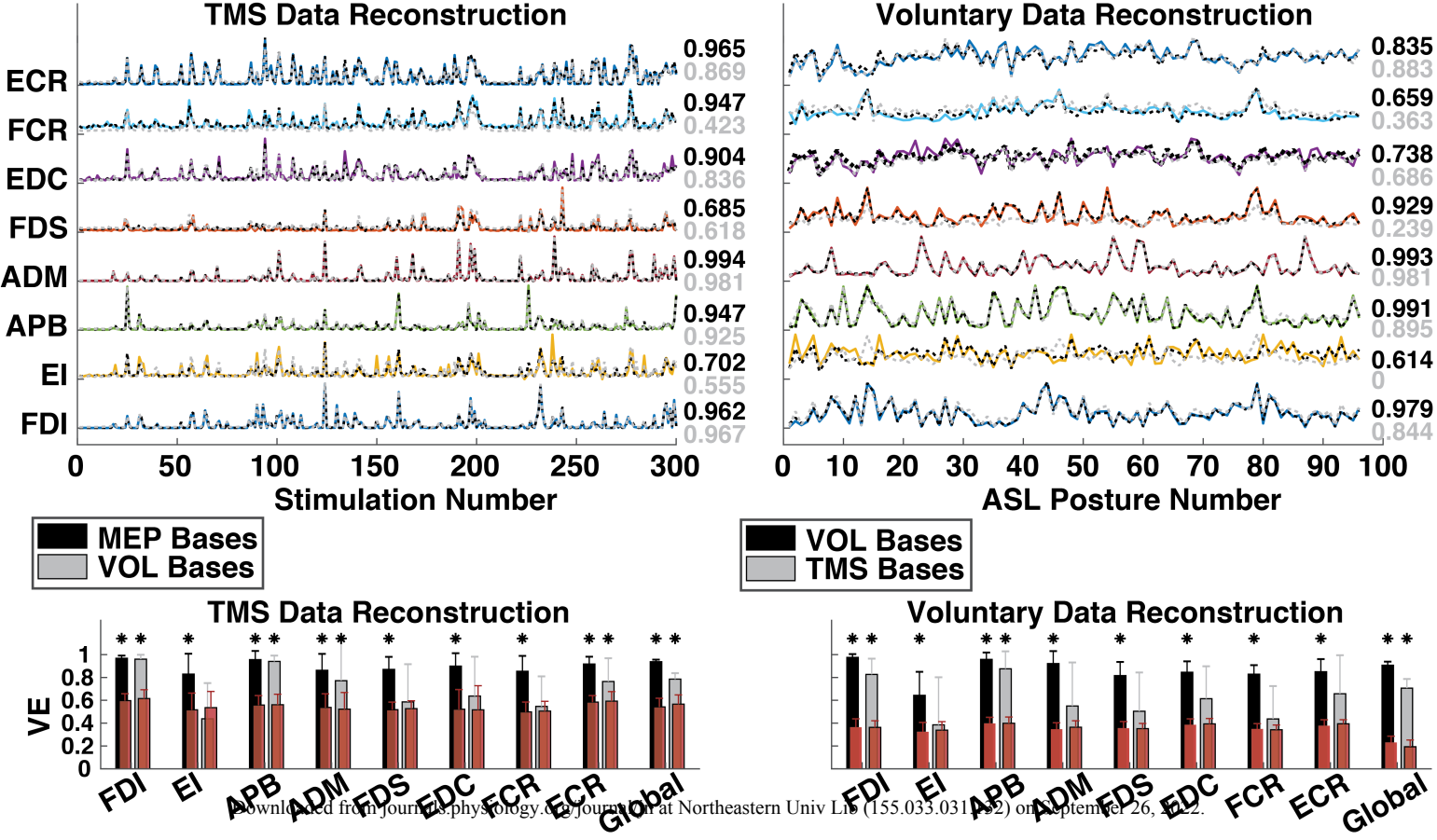

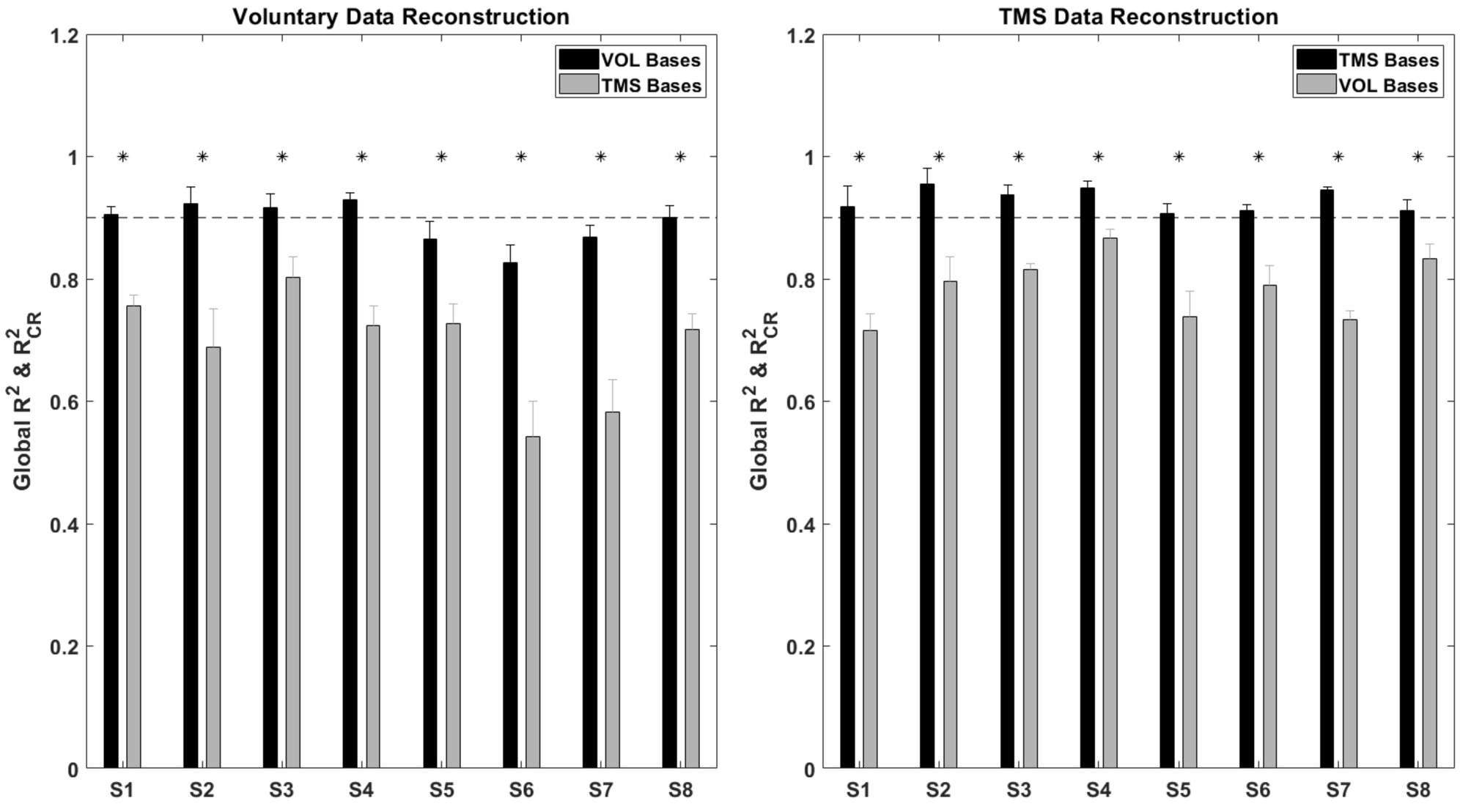

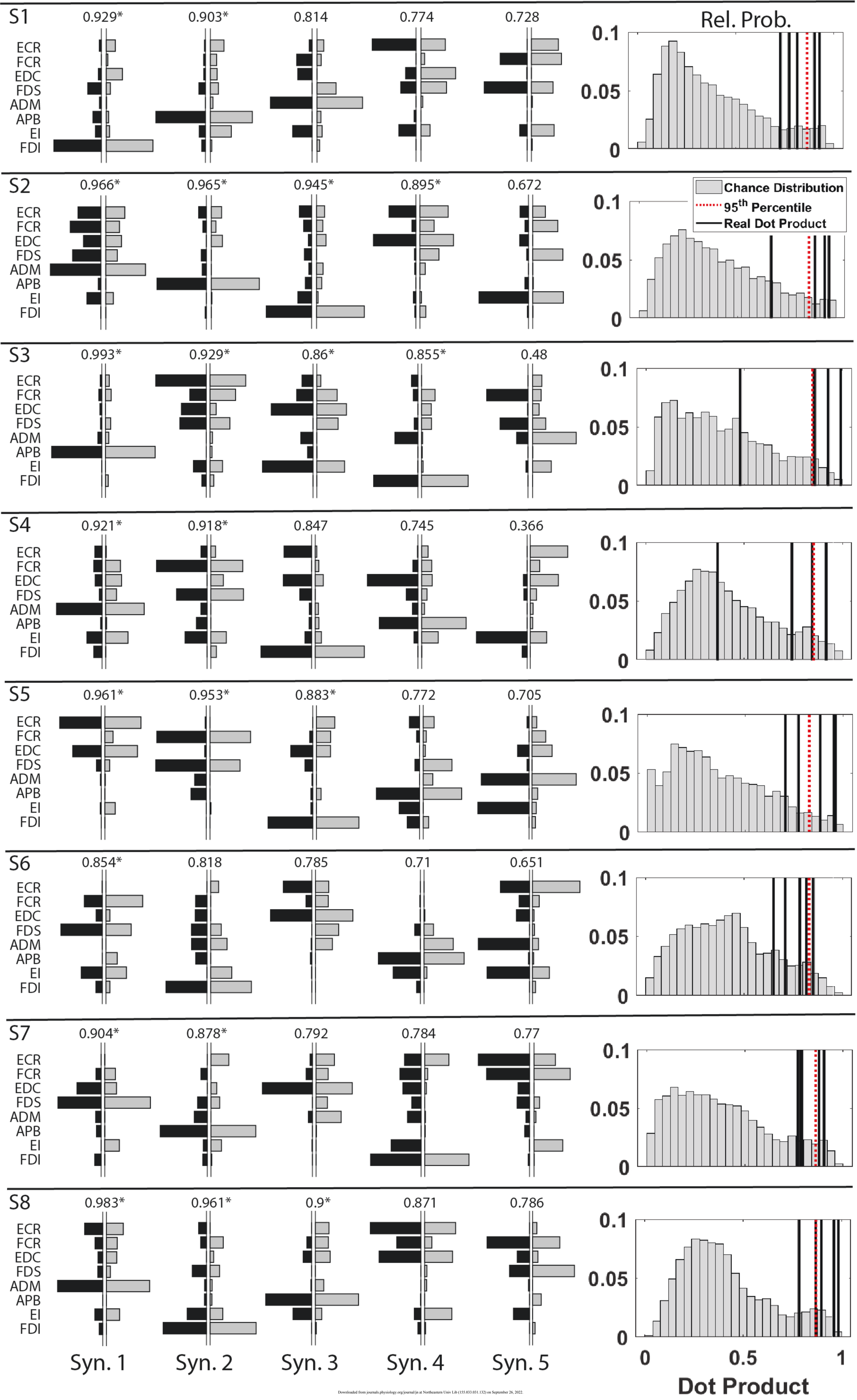

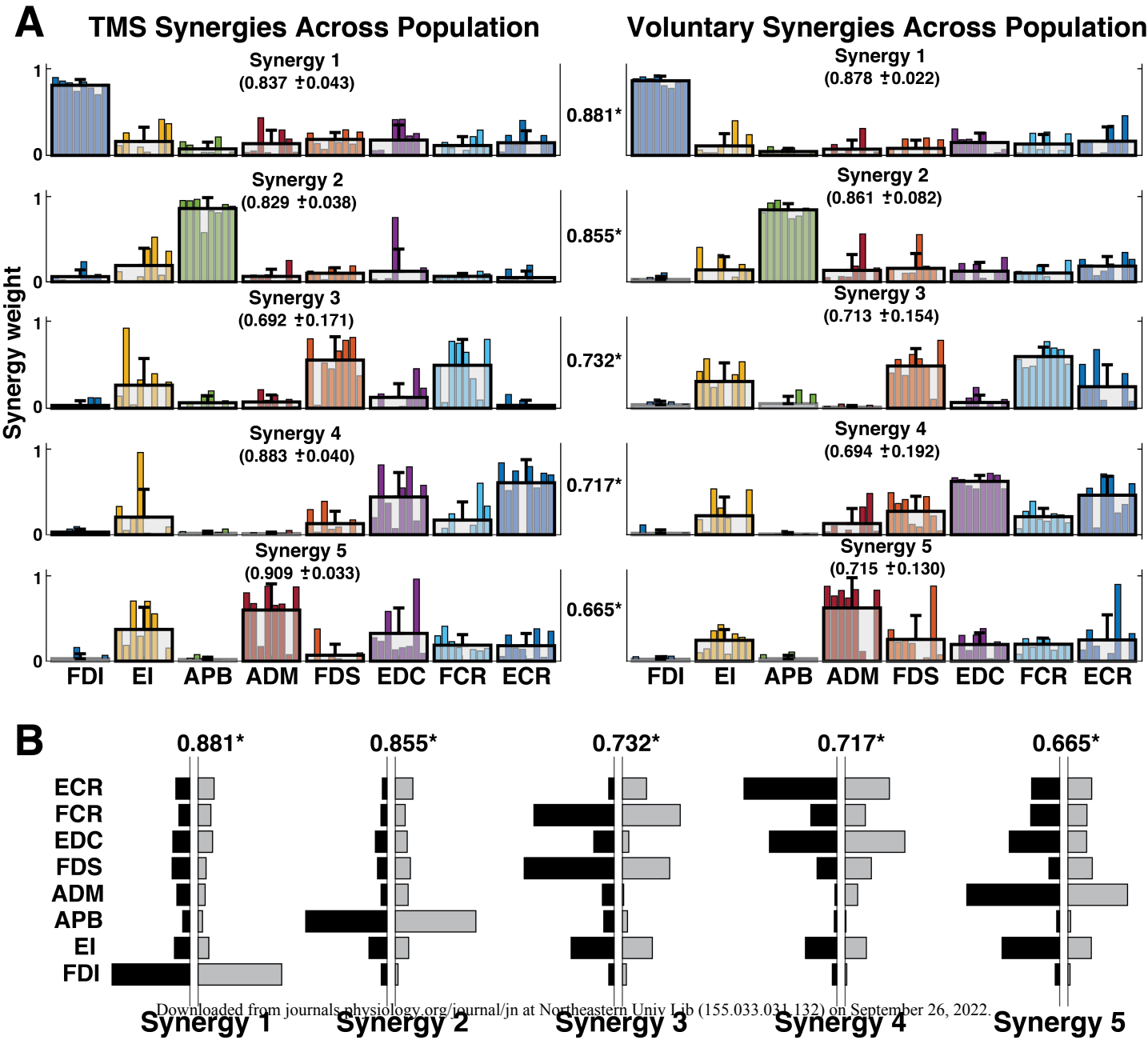

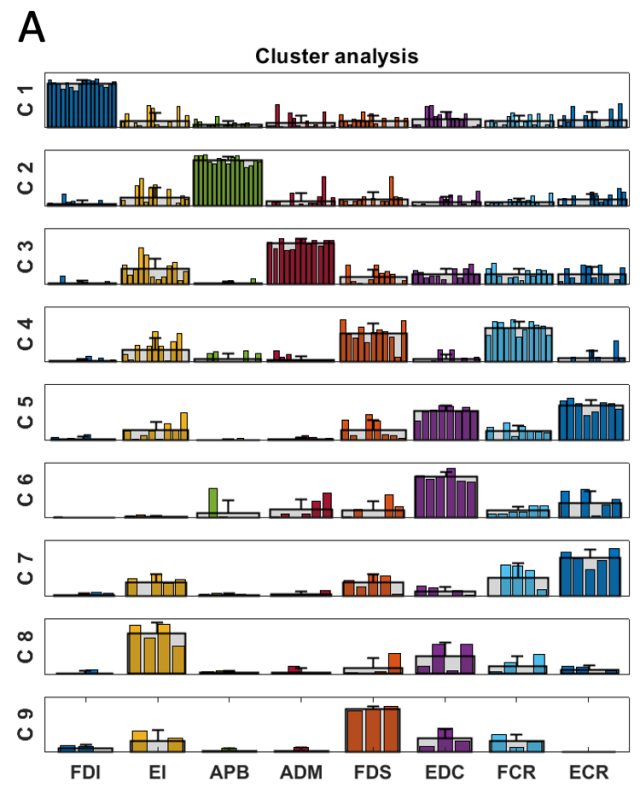

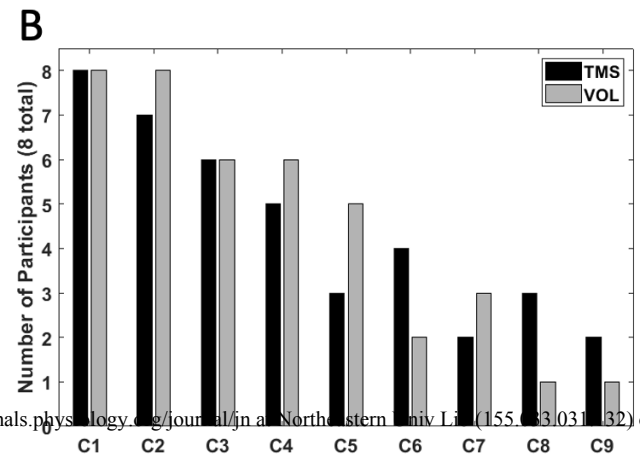

Similarity of Hand Muscle Synergies Elicited by Transcranial Magnetic Stimulation and Those Found During Voluntary Movement

METHODS

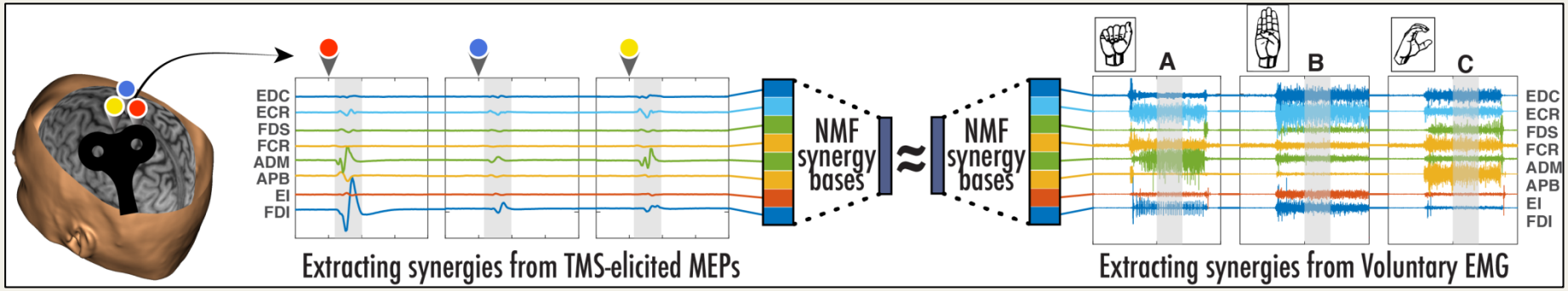

RESULTS

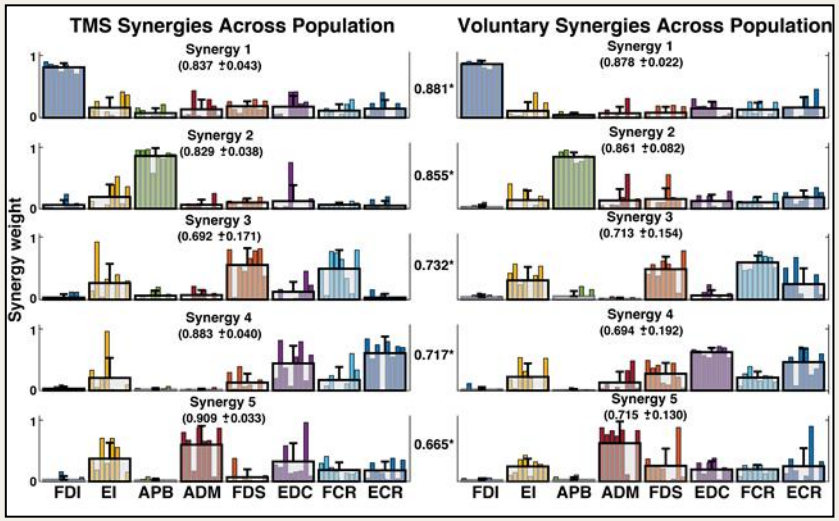

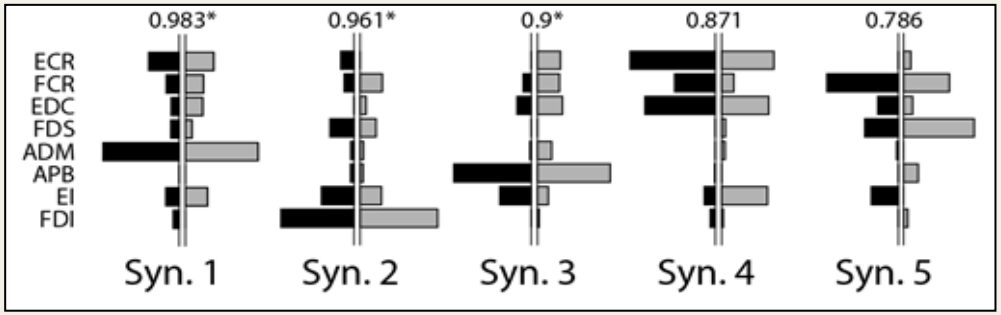

CONCLUSION Hand muscle synergies extracted from TMS-evoked MEPs resemble those extracted voluntary movement at the individual and population level.